

# Sequential Learning in the Dense Associative Memory

Hayden McAlister<sup>1</sup>, Anthony Robins<sup>1</sup>, Lech Szymanski<sup>1</sup>

<sup>1</sup>School of Computing, University of Otago, Dunedin, New Zealand.

## Abstract

Sequential learning involves learning tasks in a sequence, and proves challenging for most neural networks. Biological neural networks regularly conquer the sequential learning challenge and are even capable of transferring knowledge both forward and backwards between tasks. Artificial neural networks often totally fail to transfer performance between tasks, and regularly suffer from degraded performance or catastrophic forgetting on previous tasks. Models of associative memory have been used to investigate the discrepancy between biological and artificial neural networks due to their biological ties and inspirations, of which the Hopfield network is perhaps the most studied model. The Dense Associative Memory, or modern Hopfield network, generalizes the Hopfield network, allowing for greater capacities and prototype learning behaviors, while still retaining the associative memory structure. We investigate the performance of the Dense Associative Memory in sequential learning problems, and benchmark various sequential learning techniques in the network. We give a substantial review of the sequential learning space with particular respect to the Hopfield network and associative memories, as well as describe the techniques we implement in detail. We also draw parallels between the classical and Dense Associative Memory in the context of sequential learning, and discuss the departures from biological inspiration that may influence the utility of the Dense Associative Memory as a tool for studying biological neural networks. We present our findings, and show that existing sequential learning methods can be applied to the Dense Associative Memory to improve sequential learning performance.

## 1 Introduction

Sequential learning, sometimes continual learning or lifelong learning, is an important area of study in machine learning where models are exposed to several tasks in sequence and must learn new tasks without exposure to previous ones. Biological neural networks can perform extremely well in sequential environments, and can even use information from previous tasks to help learn new tasks quicker, “forward transfer”, and achieve better-than-random performance on unseen tasks, “zero-shot” performance. However, artificial neural networks struggle immensely in sequential environments, often forgetting previous tasks entirely (catastrophic forgetting) let alone showing any signs of forward transfer. There have been many techniques developed to improve the ability of artificial neural networks to learn sequential tasks. These include architectural methods that alter / add to the network architecture for each new task, regularization methods that create a surrogate loss term for previous tasks to use in future learning, and rehearsal based methods that replay data from previous tasks to prevent forgetting.

The Hopfield network is a well studied model of autoassociative memory. In the Hopfield network, states are learned to be attractors in an energy space such that probe states iterate towards and stabilize on them (within some constraints). Importantly, the Hopfield network has had significant presence in research bridging the gap between computer science, neuroscience, and psychology thanks to the biological inspiration of the Hopfield

network. Of particular note is the simplicity and biological plausibility of the learning algorithm – many such algorithms being based on the Hebbian learning rule where “neurons that fire together, wire together”. The Hopfield network has also been the focus of ample research on sequential learning, again thanks to the parallels between the network and biological networks. Recently, an abstraction has been developed on top of the classical Hopfield network, the interaction vertex, leading to the Dense Associative Memory, sometimes the modern Hopfield network. The previously quadratic energy wells are replaced by wells of any increasing function that become steeper with the interaction vertex. The Dense Associative Memory has been shown to have increased capacity, improved training times, and interesting memory structures compared to the classical Hopfield network. In exchange, the Dense Associative Memory loses some of the biologically plausible features of the classical network. The Hebbian learning rule, simple weight matrix, and single-step update rule are replaced by gradient descent, set of memory vectors, and a contrastive difference of similarities respectively. We discuss these trade-offs at length in Section 2.1.

Sequential learning has been studied at length in the classical Hopfield network, particularly at the intersection of psychology and computer science. Drawing parallels between the human brain and the relatively simple network has proven useful in making conclusions about biological learning processes. However, there is a distinct lack of research into sequential learning in the Dense Associative Memory. Although the changes between the Hopfield network and Dense Associative Memory make a step away from biological plausibility, it is still worth studying in the context of sequential learning as an autoassociative memory. In particular, the unique architecture compared to feed-forward networks results in interesting behaviors when using traditional sequential learning methods. In this paper we will investigate sequential learning in the Dense Associative Memory, focusing on the differences in behavior at low and high interaction vertices, the effectiveness of various state-of-the-art sequential learning methods when applied to the network, and the differences between sequential learning as an autoassociative memory and as a classifier.

## 2 Literature Review

### 2.1 The Hopfield Network

The classical Hopfield network is a relatively simple artificial neural network that operates as a model of autoassociative memory (Hopfield, 1982). Although earlier autoassociative memories exist (Steinbuch and Piske, 1963; Steinbuch, 1965; Kohonen, 1972; Kohonen, 1978), the Hopfield network is perhaps the most studied in the class. Typically, a network of dimension  $N$  operates over states that are drawn from a discrete domain, usually the binary  $\{0, 1\}^N$  or bipolar  $\{-1, 1\}^N$ . The network can be operated over a continuous domain, but it has been shown that the interesting behavior of the network is the same whether operating over continuous or discrete domains (Hopfield, 1984), and hence the simpler discrete domain is more common. The network usually employs the Hebbian

learning rule (Hebb, 1949), or a variation of the Hebbian such as the Widrow-Hof (Widrow and Hoff, 1960) or Storkey (Storkey, 1997) learning rule. The classical Hopfield network has been analyzed extensively from the perspective of statistical physics, where the model is equivalent to that of a Sherrington-Kirkpatrick spin-glass system (Amit, Gutfreund, and Sompolinsky, 1985a; Amit, Gutfreund, and Sompolinsky, 1985b; Kirkpatrick and Sherrington, 1978; Bovier and Niederhauser, 2001). The long range spinglass is a mature model with well studied classes of states, phase transitions, and dynamics which can all be applied nearly directly to the Hopfield network, although statistical physics rarely looks at the equivalent of sequential learning. The Hebbian learning rule has been shown to give rise to a network capacity of only  $0.14N$  states from both the computer science (McEliece et al., 1987; Hertz, 1991) and physics perspectives (Amit, Gutfreund, and Sompolinsky, 1985b; Amit, Gutfreund, and Sompolinsky, 1987). This makes the classical Hopfield network difficult to work with, as the linear network capacity is made impractical by the quadratic weight matrix size  $N^2$ . More relevant to our work, there has been significant analysis of the network in the field of psychology thanks to its biological plausibility (Amit, 1994; Maass and Natschlager, 1997; Tsodyks, 1999; Hopfield, 1999). Of note is the work on prototype formation in the Hopfield network, which may help explain prototype learning in the human brain (Robins and McCallum, 2004; McAlister, Robins, and Szymanski, 2024b).

The Dense Associative Memory abstracts the Hopfield network by effectively allowing variation in the steepness of the energy wells forming the attractor space (Krotov and Hopfield, 2016). This is done by altering a hyperparameter known as the interaction vertex  $n \in \mathbb{R}^+$ . It has been shown that the Dense Associative Memory has the same behavior as the classical network for  $n = 2$  (Krotov and Hopfield, 2016; Demircigil et al., 2017), meaning the modern network could in theory replace the classical network in all results. However, the modern network has carved its own distinct niche thanks to several other alterations. The shift from a Hebbian based learning rule to a gradient descent has removed a significant portion of the biological plausibility (Stork, 1989), making the network potentially less attractive in the study of psychology and neuroscience. This is compounded by a change from a weight matrix (which can describe the connection strength between a set of  $N$  neurons) to a set of memory vectors that are isolated from one another. However, as a model of autoassociative memory, the gains to the network capacity are hard to ignore. Specifically, Krotov and Hopfield find a network capacity of:

$$\frac{1}{2(2n-3)!!} \frac{N^{n-1}}{\ln(N)},$$

meaning the network capacity is superlinear for  $n > 2$ . Furthermore, the network memories have been observed to have interesting behaviors between low and high interaction vertices. The memories appear to take on feature-like values at low interaction vertices, but transition to prototype-like values at high interaction vertices, indicating the network is learning to model the training data differently as the interaction vertex changes. This is entirely different to the prototype behavior observed in the classical Hopfield network, which

emerges from properties of the Hebbian learning rule (McAlister, Robins, and Szymanski, 2024b).

Despite the steps away from biological plausibility, the Dense Associative Memory has still been used in studies of psychology and neuroscience, with links made to the human brain (Snow, 2022; Checiu, Bode, and Khalil, 2024). The main focus of research around the Dense Associative Memory recently, however, has been on the correspondence to the attention mechanism used in transformers and Large Language Models (Vaswani et al., 2017; Ramsauer et al., 2021). This shows there is an interest in autoassociative memories and the possibility for biologically plausible explanations of network mechanics. Moreover, LLMs and attention based models often undergo a fine-tuning step in which the model learns on a small set of data corresponding to a new, specific task without retraining on the massive amount of general data seen previously. This is very similar to a sequential learning environment, and our work may have consequences for how fine-tuning is applied in the Dense Associative Memory equivalent attention mechanism.

## 2.2 Sequential Learning in the Hopfield Network

The classical Hopfield network has been studied in sequential learning environments at length, alongside other network architectures. Nadal et al. (Nadal et al., 1986) analyzed the recall of the Hopfield network after training on a sequence of items. The weights of the network were rigorously analyzed as new items were added, and the magnitudes associated with each item were quantified. Notably, Nadal et al. found results that are strikingly similar to the spin glass literature (Amit, Gutfreund, and Sompolinsky, 1985b; Toulouse, Dehaene, and Changeux, 1986; Personnaz et al., 1986). Notably, the catastrophic forgetting observed when the network’s capacity is exceeded is linked directly to an item’s associated weight magnitude dropping below a derived threshold — something that occurs nearly simultaneously for all stored items above the network capacity. Burgess et al. (Burgess, Shapiro, and Moore, 1991) investigate list-learning in the Hopfield network, a form of sequential learning where items are presented one at a time for a single epoch, effectively forming tasks of a single item. Recall is tested over all previously presented items at the end of each epoch. Burgess found the accuracy is high for both early and late items, but lower for intermediate items. This was linked to the biological memory model of short-term and long-term memory (Shiffrin and Atkinson, 1969) as well as the concepts of recency and primacy/familiarity (Lund, 1925). Burgess et al. also experimented with small modifications to the learning algorithms in the Hopfield network, such as increasing weights in proportion to the weight magnitude. Thanks to the simplicity of Hebbian learning rules, this is effectively equivalent to rehearsal in this domain. When using this method, it was found that the network could be tuned to exhibit strong primacy or strong recency behavior easily, and with some difficulty both behaviors could be observed.

Robins investigated a more explicit form of rehearsal, looking at feed-forward neural networks with new tasks alongside items from previous tasks. Of particular interest are the

variations on rehearsal studied. Sweep rehearsal (Robins, 1993) involves rapidly updating the items rehearsed from some larger buffer of previous task items, which should provide a constant error signal for the new task every batch, while the rehearsal error signal is effectively smoothed out over many batches. Robins found this resulted in better sequential learning performance when using sweep rehearsal compared to traditional buffer rehearsal. However, it was also found that in feed-forward networks the learned behavior was to “pass-through” items rather than specifically learning the task items, limiting the usefulness of these techniques for sequential learning. Pseudorehearsal (Robins, 1995) is another variation of rehearsal based techniques, where buffer items are not sampled from previous tasks but instead from the network itself. Pseudorehearsal is described at length in Section 3, but effectively alleviates catastrophic forgetting without requiring access to previous task data by probing the network with random inputs and using the resulting output as a buffer item — something that has been proposed to model the function of dreaming in memory consolidation in the human brain. Later Robins and McCallum moved from feed-forward networks to the Hopfield network (Robins and McCallum, 1998). In particular, rehearsal based mechanisms were implemented in the Hopfield network, and for the first time sequential learning in a batched environment was studied in the Hopfield network (in contrast to list learning, such as in (Burgess, Shapiro, and Moore, 1991)). Using the thermal perceptron learning rule (Frean, 1992) rather than the Hebbian learning rule (which, as discussed above, implements sequential learning inherently), Robins and McCallum are able to push past the performance caps previously set by the low network capacity associated with Hebbian learning, and find that catastrophic forgetting still occurs but now in a similar fashion to feed-forward networks; later batches “wipe out” earlier ones. Robins and McCallum also showed that pseudorehearsal improved the sequential learning performance of the Hopfield network, particularly when the generated items are representative of the actual task items.

In contrast to the work done on sequential learning in the classical Hopfield network, there has been very little on sequential learning in the Dense Associative Memory. Indeed, it is still unknown how traditional sequential learning methods perform in combatting catastrophic forgetting, or how the interaction vertex effects forgetting. This paper aims to fill that gap and investigate the broad foundations of sequential learning in the Dense Associative Memory.

## 2.3 Sequential Learning Datasets

There are a variety of sequential learning datasets that are standard across the literature. A decent amount of sequential learning has focused on classification tasks, as these networks were and are prevalent in the current age of machine learning. Some such datasets have been based around well known, widely available datasets such as MNIST digit classification (LeCun, Cortes, and Burges, 1998) and CIFAR (Krizhevsky and Hinton, 2009). These are image based classification datasets which proved popular during the rise of image

classifications models after AlexNet (Krizhevsky, Sutskever, and Hinton, 2012). To convert these to sequential learning datasets, the original data is split in some way into a series of tasks. The degree to which different tasks are related to one another may vary depending on what the aspect of learning is being focused on; for example, forward and backwards transfer may want tasks that are highly related, while capacity investigations may want entirely unrelated tasks. Common MNIST variations include Rotated MNIST (in which images are rotated by some amount, disrupting the data very little and leading to highly related tasks) and Permuted MNIST (Kirkpatrick et al., 2017) (in which the pixels of images belonging to one task are permuted some amount, leading to entirely unrelated tasks, effectively an entire new MNIST dataset for each task). Another common transformation is to take only some of the classes of the dataset in each class. This is commonly seen in Split CIFAR-10 and Split CIFAR-100 (Zenke, Poole, and Ganguli, 2017), as the structure of the CIFAR dataset does not lend itself to permutation without the tasks being extremely large. Split MNIST (Goodfellow et al., 2015) is also well known.

Recently, perhaps in tandem with growing hardware power, other datasets have become more popular in a sequential learning environment. CUB (Welinder et al., 2010) and AWA (Lampert, Nickisch, and Harmeling, 2009) have both seen use in sequential learning (Chaudhry et al., 2019) as Split CUB and Split AWA. With the rise of transformers, attention, and Large Language Models, sequential learning over natural language datasets has also become common (Houlsby et al., 2019; Douillard et al., 2022; Li et al., 2022). Again, these datasets are usually derived from well known natural language datasets, although with more of a focus on classification tasks. Examples of NLP sequential learning datasets are Split Reuters (news article classification) (Lewis et al., 2004), Split Wiki-30K (Wikipedia article classification) (Zubiaga, 2012), and Split Arxiv (Arxiv paper classification) (Yang et al., 2018).

Although the Dense Associative Memory has been generalized to take continuous values (Ramsauer et al., 2021), we are looking to investigate sequential learning in the most basic of the network architectures. This will allow us to measure if the adjustment of the interaction vertex alone impacts sequential learning, without possible interference of other factors such as the alterations that allow for the continuous network. Therefore, we will use the binary-valued Dense Associative Memory as first proposed by Krotov and Hopfield (Krotov and Hopfield, 2016) with modifications that provably do not alter the original network properties (McAlister, Robins, and Szymanski, 2024a). This paper will focus on binary datasets (or datasets that can be thresholded without loss of information), such as Permuted MNIST and Rotated MNIST.

### 3 Sequential Learning Methods

Sequential learning methods can be broadly classified into three categories: architectural, rehearsal, regularization. Architectural sequential learning methods make some change to

the network architecture in an attempt to improve the sequential learning performance of the network. This may include freezing specific weights that are important to previous task, avoiding forgetting by preventing those weights from changing, or adding new modules to the network that are able to fit new tasks, minimizing disruption to previous tasks. Rehearsal-based sequential learning methods keep a buffer of items associated with previous tasks to replay during training of the next task. This ensures an error signal is still present from previous tasks and allows a model to weigh learning new data against forgetting old data. Finally, regularization-based methods introduce a surrogate term to the loss function that models the true loss of previous tasks, as if we still had access to the previous items. These methods can be more efficient than rehearsal-based methods, due to the lower memory overhead and effectively smaller amount of data, but requires a good approximation of the previous task’s loss function to operate effectively. Moreover, most regularization-based techniques approximate the loss with a quadratic term; a good approximation near a minima of the previous task loss, but ignores the existence of other well-performing minima. Below, we discuss in detail the specific methods we will investigate.

### 3.1 Naive Rehearsal

The first method we will investigate is by far the simplest — naive rehearsal. While rehearsal-based methods may appear simple at first glance, there is some depth to these methods. The buffer items need not be taken directly from the training data of previous tasks and could instead be generated another way, meaning the assumption of access to previous tasks is not violated. Furthermore, the method in which rehearsal items are introduced during training may vary, from naively introducing the entire buffer at each epoch to sampling a new mini-buffer that is updated every epoch, known as sweep-rehearsal (Robins, 1995; Silver, Mason, and Eljabu, 2015).

In naive rehearsal we take some proportion of the previous task items and store them in a buffer to introduce during the next task’s training. We take a constant proportion across all tasks, e.g. 100 items from task one, 100 from task two, and so on. Typically, some predefined buffer size is used, and the buffer is utilized entirely throughout learning (i.e. initially the entire buffer are items from the first task, after task two the buffer is half items from task one, half from task two, and so on). However, we found excellent results using a growing buffer, with considerably shorter training times. Our rehearsal implementation combined the buffer with the new task data, then shuffled and batched this. This means individual buffer items are seen as frequently as individual new items — once per epoch — and effectively implements a type of sweep rehearsal (as the buffer items are newly sampled each batch). We may be able to save some memory by replaying the same buffer items more than once, but our investigation here is foundational, and hence the best-case scenario with a large number of buffer items is still interesting. We parameterize naive rehearsal using the rehearsal proportion: a rehearsal proportion of 1.0 would be to present

the entire previous task alongside the new task, while 0.1 would be to present only 10% of the previous task items. We will investigate the effects of different rehearsal proportions on the sequential learning performance of the Dense Associative Memory.

### 3.2 Pseudorehearsal

Pseudorehearsal (Robins, 1993; Robins, 1995), similar to naive rehearsal above, is a rehearsal-based sequential learning method. In pseudorehearsal, however, buffer items are not sampled from the training data of previous tasks, but instead from randomly generated data that is fed through the model. This removes the need for access to the previous training data, as only the model itself is required to generate buffer items. Pseudorehearsal has been studied in the Hopfield network (Robins and McCallum, 1998), both using both homogenous (a random state is relaxed to a stable point, which is taken as the buffer item) and heterogeneous methods (a random state is relaxed to a stable one, and the *pair* is taken as a buffer item to ensure the mapping remains consistent during training of the next task). We will focus on the homogenous method. After each task, we will generate some number of random probes (based on the amount of training data in the previous task, so we can compare the buffer size to the rehearsal method above) and relax these probes to a stable state. We then treat these relaxed probes exactly as if they were sampled from the training data using naive rehearsal — combine with the data for the next task, shuffle, batch, and train.

We theorize that pseudorehearsal will be extremely effective at higher interaction vertices. It is known that the memories of the Dense Associative Memory undergo a feature to prototype transition as the interaction vertex is raised (Krotov and Hopfield, 2016; Krotov and Hopfield, 2018). When the memories are learned to be prototypes of the training data, we expect random probes to stabilize on or near those prototype states, meaning we get buffer items that are extremely representative of the previous task training data without requiring explicit access to the data itself. This should improve the efficacy of pseudorehearsal, which has always suffered from buffer items that are not representative of training data (Atkinson et al., 2021).

### 3.3 Gradient Episodic Memories

The following methods are somewhat hybrid regularization and rehearsal-based methods. Gradient Episodic Memories (Lopez-Paz and Ranzato, 2022) aims to preserve performance on previous tasks by ensuring the gradient vector of the loss on the current task never points against the gradient of the loss on previous tasks. To measure the gradient on previous tasks, a buffer of previous task items is kept and evaluated each batch to find the gradients. Therefore, Gradient Episodic Memories *regularizes* the weight updates by *rehearsing* previous task items. One of the main benefits of GEM over other sequential learning methods, particularly the quadratic-penalty weight-importance methods we discuss below,

is the explicit allowance of improvement on previous tasks. Because the gradient of the loss is allowed to point in the same direction as previous task’s losses, this allows the model to update weights away from the optimal weights found at the end of the previous task as long as the update is believed to improve the loss on that previous task (rather, improve the loss on the buffer sampled from the previous task). The motivation for this difference in behavior is to allow for backwards transfer, where future tasks can improve performance on previous tasks, something that is much more difficult to achieve when weight updates are penalized significantly.

Lopez-Paz and Ranzato alter the typical learning objective with constraints on previous task performance:

$$\begin{aligned} & \text{minimize}_{\theta} && \mathcal{L}(\theta, X_{\mu}) \\ & \text{subject to} && \mathcal{L}(\theta, \mathcal{M}_{\nu}) \leq \mathcal{L}(\theta_{\mu-1}, \mathcal{M}_{\nu}) \text{ for } \nu < \mu, \end{aligned} \quad (1)$$

that is, minimize the current task loss  $\mathcal{L}(\theta, X_{\mu})$  as long as the loss on the previous task’s buffer  $\mathcal{M}_{\nu}$  does not increase with respect to the start of the current task. Here,  $\mathcal{L}$  is the base loss, as no surrogate loss terms are introduced. Notably, we do not need to store the entire old model as long as we store just the loss on the buffer items. This objective can be optimized while respecting the constraints by observing that if the gradient of the loss points in the opposite direction to any previous task’s gradient, we project the current gradient on to the closest vector that doesn’t. Formally, to get the projected gradient  $\tilde{g}$  from the original gradient  $g$  and gradients on previous tasks  $g_{\nu}$  we solve another optimization problem:

$$\begin{aligned} & \text{minimize}_{\tilde{g}} && \frac{1}{2} \|g - \tilde{g}\|_2^2 \\ & \text{subject to} && \langle \tilde{g}, g_{\nu} \rangle \geq 0 \quad \forall \nu < \mu. \end{aligned} \quad (2)$$

We can express this as a quadratic programming problem of the number of parameters in the network:

$$\begin{aligned} & \text{minimize}_z && \frac{1}{2} z^{\top} z - g^{\top} z + \frac{1}{2} g^{\top} g \\ & \text{subject to} && Gz \geq 0, \end{aligned} \quad (3)$$

Where  $G = (g_1, g_2, \dots, g_{\mu-1})$ . The constant term  $g^{\top} g$  is discarded. However, since the network is likely to have many parameters, this problem is often intractable to solve, so we shift the problem to the dual space, which has only  $\mu - 1$  variables instead:

$$\begin{aligned} & \text{minimize}_v && \frac{1}{2} v^{\top} G G^{\top} v + g^{\top} G^{\top} v \\ & \text{subject to} && v \geq 0. \end{aligned} \quad (4)$$

Once we solve this problem to find  $v^*$ , we can get the projected gradient vector:

$$\tilde{g} = G^{\top} v^* + g, \quad (5)$$

which we can use for weight updates as usual.

While GEM is theoretically sound, its main issue comes with an increasing number of constraints as the number of tasks grows. Every new task adds a new constraint to the primal problem, which in turns adds a new parameter to the dual problem that is actually solved. These increasingly limit the directions in which the projected gradient is allowed to point, potentially leading to very poor learning on new tasks when the number of previous tasks is large. However, for large networks the curse of dimensionality means the number of directions is extremely large, so this is not as significant a problem as it may seem. To find the vector  $G$ , we must compute the gradient on a buffer of items from the previous task, which is also computationally expensive, and requires us to store a buffer of items like a rehearsal-based task. We will again parameterize this method using a rehearsal proportion hyperparameter to see how different buffer sizes impacts the sequential learning performance of the model. On a practical note, quadratic programming solvers are typically iterative and implemented on the CPU, meaning the GPU bound model gradients must be transferred to the CPU, used in the optimization for  $v^*$ , and transferred back to the GPU for use in gradient descent, which is tremendously expensive when performed every batch.

### 3.4 Averaged Gradient Episodic Memory

Average Gradient Episodic Memory (Chaudhry et al., 2018) aims to solve some of the issues with Gradient Episodic Memories above by relaxing the conditions on the optimization problems. Rather than requiring that the projected gradient does not point against *any* previous task’s gradient, leading to one constraint per previous task, we require the projected gradient to not point against the gradient of *all* previous tasks *simultaneously*. That is, rather than having a gradient per previous task, we have a single gradient after running the model on all tasks. This is the *average* in Averaged Gradient Episodic Memory. By reducing the number of constraints to one, we also greatly reduce the computation required to find the projected gradient  $\tilde{g}$ ; in fact, a closed form solution for this optimization problem exists. However, by only constraining the gradient to point in the same direction as the gradient on the combined task buffers we may allow learning that goes against the gradient for an individual task, potentially leading to forgetting, but only if the learning would benefit all previous tasks *on average*.

A-GEM looks to learn a new task with the objective:

$$\begin{aligned} & \text{minimize}_{\theta} && \mathcal{L}(\theta, X_{\mu}) \\ & \text{subject to} && \mathcal{L}(\theta, \mathcal{M}_{\mu}) \leq \mathcal{L}(\theta_{\mu-1}, \mathcal{M}_{\nu}) \text{ where } \mathcal{M}_{\mu} = \cup_{\nu < \mu} \mathcal{M}_{\nu}. \end{aligned} \tag{6}$$

Note by combining the individual task buffers  $\mathcal{M}_{\nu}$  into a single buffer  $\mathcal{M}_{\mu} = \cup_{\nu < \mu} \mathcal{M}_{\nu}$  we enforce only a single constraint. The projected gradient is then given by:

$$\begin{aligned} & \text{minimize}_{\tilde{g}} && \frac{1}{2} \|g - \tilde{g}\|_2^2 \\ & \text{subject to} && \langle \tilde{g}, g_{\mu} \rangle \geq 0, \end{aligned} \tag{7}$$

where  $g_\mu$  is the gradient on the buffer  $\mathcal{M}_\mu$ . This optimization problem is much simpler than the one in Equation 2 and does not require the dual space problem and expensive quadratic programming solvers. Instead, the closed form solution of Equation 7 is:

$$\tilde{g} = g - \frac{g^\top g_\mu}{g_\mu^\top g_\mu} g_\mu. \quad (8)$$

The closed form is simple enough to be implemented entirely on the GPU, avoiding the computation problems of GEM above, although we must still compute the gradient on the previous task buffers.

### 3.5 L2 Regularization

Regularization-based methods add an additional term to the loss function that approximates the previous task’s loss. Usually that additional term is proportional to the squared difference of the previous task’s optimal weights and the current weights, meaning large shifts from the previous optimal weights are penalized heavily. Many regularization-based methods include a measure of weight importance to allow “unimportant” weights to shift more than “important” ones. We will investigate several such regularization methods with weight importance measures, but as a sanity check we will also investigate the degenerate case of assigning an equal importance to every weight. This is functionally equivalent to L2 regularization, also called weight decay.

Formally, this class of quadratic term regularization methods look like

$$\mathcal{L}(\theta) = \mathcal{L}_{\text{Base}}(\theta) + \lambda \sum_{\mu} \sum_k \omega_{k,\mu} (\theta_{k,\mu}^* - \theta_k)^2, \quad (9)$$

where  $\mathcal{L}_{\text{Base}}(\theta)$  is the base loss on the next task (e.g. mean squared error, binary cross entropy, ...),  $\mu$  indexes over tasks,  $k$  indexes over the weights of the model,  $\omega_k$  is the importance of  $\theta_k$ , and  $\theta_{k,\mu}^*$  is the optimal value of  $\theta_k$  found at the end of the previous task.  $\lambda$  is a hyperparameter to weigh between learning the new task (low  $\lambda$ ) and remembering the old task (high  $\lambda$ ). Some methods include a new quadratic term for each task completed, therefore also including another importance and optimal weight value too. In L2 regularization, we set  $\omega = 1$  for each weight, and include a new quadratic term, with optimal weights  $\theta_{k,\mu}^*$ , after each task.

### 3.6 Elastic Weight Consolidation

Elastic Weight Consolidation (Kirkpatrick et al., 2017) is the first regularization-based technique we will discuss with a nontrivial weight importance measure. In EWC, weight importance is measured using the Fisher information matrix of the network parameters, effectively quantifying how each parameter affects the prediction for a sample of the training data. The presence of previous task items means that this calculation must be done

either with a buffer of previous task items (in which case, rehearsal methods may be more effective) or at the end of the task (i.e. it is known the model is to undergo sequential learning). The Fisher information matrix has several useful properties for this application (Pascanu and Bengio, 2014), the most important of which are that it can be computed from the first derivative of the loss, and it approaches the second order derivative of the base loss function near a minima. The first property allows us to calculate the Fisher information matrix efficiently, as directly computing the second derivative of a large model is often extremely expensive if not entirely intractable. The second property allows us to approximate the minima of the loss provably effectively without having to directly measure the second derivative.

Over a sample of training data the Fisher information matrix, and hence the weight importance, is approximated by:

$$\omega_k = \left( \frac{\partial}{\partial \theta_k} \mathcal{L}_{\text{Base}}(\theta) \right)^2. \quad (10)$$

Aich (Aich, 2021) has a good discussion and formalization of the derivation of this approximation.

The loss function on future tasks is defined by:

$$\mathcal{L}(\theta) = \mathcal{L}_{\text{Base}}(\theta) + \frac{\lambda}{2} \sum_{\mu} \sum_k \omega_{k,\mu} (\theta_{k,\mu}^* - \theta_k)^2. \quad (11)$$

Note in EWC we have a quadratic term for each completed task, indexed by  $\mu$ , rather than a single term that is carried through. The additional factor of  $\frac{1}{2}$  on the  $\lambda$  is included for consistency with the original literature.

### 3.7 Memory Aware Synapses

Memory Aware Synapses (Aljundi et al., 2018) is another weight importance regularization-based sequential learning technique. In contrast to EWC, which uses the Fisher information and the loss function of the task, MAS measures the model sensitivity directly. A Taylor expansion of the model output with respect to each network parameter gives a weight importance measure of:

$$\omega_k = \frac{1}{N} \sum_{i=1}^N \left\| \frac{\partial F(X, \theta)}{\partial \theta_k} \right\|, \quad (12)$$

again for a sample of the training data  $X$ . Note the network output  $F(X, \theta)$  itself is used, not the loss function  $\mathcal{L}_{\text{Base}}(\theta)$ . The gradient with respect to each possible network output is taken and averaged, indicated by the sum over  $N$  (e.g. for a task with 10 outputs / classes,  $N = 10$ ). The value of  $\omega_k$  is accumulated over each task, so we keep some information

about previous task’s weight importances without requiring a new term per task, as in EWC.

Aljundi et al. note a slightly more efficient implementation of this technique for models with many outputs. Rather than taking the derivative of each output with respect to the model parameters, i.e. one expansion per output, instead take the Taylor expansion of the squared L2 norm of the model output as a vector. This results in only a single expansion and hence much less computation for the same result.

The modified loss used by each task is:

$$\mathcal{L}(\theta) = \mathcal{L}_{\text{Base}}(\theta) + \lambda \sum_k \omega_k (\theta_k^* - \theta_k)^2. \quad (13)$$

Unlike L2 Regularization and EWC, the single tensor of optimal weights  $\theta_k^*$  is updated with each task, as are the weight importances  $\omega_k$ .

### 3.8 Synaptic Intelligence

Synaptic Intelligence (Zenke, Poole, and Ganguli, 2017) is a sequential learning technique again focused around a quadratic regularization term with weight importances. The importance measure is now based on the path integral of the task’s gradient along the path through parameter space taken during training. Formally:

$$\omega_{k,\mu} = \int_{t_{\mu-1}}^{t_\mu} \frac{\partial \mathcal{L}_{\text{Base}}(\theta(t))}{\partial \theta_k(t)} \frac{d\theta_k(t)}{dt} dt, \quad (14)$$

where again, the task is indexed by  $\mu$ , and the model parameters  $\theta$  dependence on time represents the changes made by training the model. Here,  $t_\mu$  indicates the time step (be that in batches or epochs) when we finish training on task  $\mu$ , so the interval  $[t_{\mu-1}, t_\mu]$  represents the training on task  $\mu$ . In practice, we approximate the continuous path integral with steps taken each epoch or batch:

$$\omega_{k,\mu} = \sum_{t=t_{\mu-1}}^{t_\mu} \frac{\partial \mathcal{L}_{\text{Base}}(\theta(t))}{\partial \theta_k(t)} (\theta_k(t) - \theta_k(t-1)). \quad (15)$$

At the end of each task, we also note the total displacement of each parameter over the course of learning that task

$$\Delta_{k,\mu} = \theta_k(t_\mu) - \theta_k(t_{\mu-1}). \quad (16)$$

We combine the weight importances of all previous tasks into a single term,

$$\Omega_{k,\mu} = \sum_{\nu < \mu} \frac{\omega_{k,\nu}}{(\Delta_{k,\nu})^2 + \epsilon}, \quad (17)$$

where  $\epsilon$  is a small constant to aid in numerical stability. The combined importance measure is then used in a single quadratic surrogate term for task  $\mu$ :

$$\mathcal{L}(\theta) = \mathcal{L}_{\text{Base}}(\theta) + \lambda \sum_k \Omega_{k,\mu} (\theta_{k,\mu}^* - \theta_k)^2 \quad (18)$$

Synaptic Intelligence is similar to Memory Aware Synapses in that the optimal weights  $\theta_{k,\mu}^*$  are updated every task, unlike Elastic Weight Consolidation which has a new set of optimal weights for each task. This can help with memory overhead, particularly for very large models, however it also means we lose some information on previous tasks. Unlike Memory Aware Synapses, which accumulates all importance measures from previous tasks into a single matrix, Synaptic Intelligence holds information about previous tasks separately, and combines these measures into an aggregate measure  $\Omega_\mu$  weighted by the total displacement of each weight in a task. We can compare these three similar methods by observing that Elastic Weight Consolidation uses the most information about previous tasks (as all weight importances are introduced in separate quadratic terms), Synaptic Intelligence uses less (combining each weight importance into one quadratic term, but weighted by the total displacement), and Memory Aware Synapses less information again (simply summing the importances of each task). L2 Regularization is the baseline method, with zero information on the weight importances or tasks. However, information quantity alone is not a good evaluation of these methods, as the derivation of the weight importances is very different between these methods and may result in better performance with less information.

## 4 Hyperparameter Tuning and Experiment Design

### 4.1 Experimental Design

In our experiments, we consistently use a series of five permuted MNIST tasks. For hyperparameter tuning we use tasks consisting of 2000 items, and for the final results we use 10000 items per task. Items are randomly sampled from the full MNIST dataset. We do not train on the full MNIST dataset in each task due to computational constraints. We use only five tasks due to instability of the network with additional training — as the number of tasks is increased, we found the network weights fluctuate increasingly wildly. We found decreasing the learning rate and / or increasing the momentum helped reduce this unwanted behavior, but at the cost of sequential learning performance.

Each task has 20% of its data set aside for validation, with the remaining 80% used for training. Each task has a different randomly generated permutation of pixels such that the classification of digits must be learned from scratch each time. We encode these items into binary vectors by flattening the pixel values into a vector, to which we append a one-hot encoded task ID, and ten neurons to represent the classes of digits. To conform to the literature that uses this dataset with the Dense Associative Memory (Krotov and Hopfield,

2016; Krotov and Hopfield, 2018), we update only the ten neurons corresponding to the class of the probe item, and updated these neurons only once. We do not use the feed-forward equivalent network in this literature, however, keeping the autoassociative memory architecture throughout our experiments.

We present the tasks to a Dense Associative Memory with 512 memory vectors for 500 epochs each. 512 memory vectors balances network performance with computing resources, and was the start of a plateau of performance as we increase the number of vectors. After training, the network relaxes the validation data and measures the validation F1 score. To ensure our random sampling of data is not biasing our results, we use average F1 score in place of accuracy, so any class imbalances are accounted for. However, we refer to accuracy throughout our discussions as the metrics are effectively the same for such large sample sizes. The two measures we use throughout our experiments are individual task accuracy and average accuracy (Caccia et al., 2021) on all tasks. The average accuracy of a series of sequential learning tasks is defined as the accuracy of all tasks seen so far  $\nu \leq \mu$  after training on task  $\mu$ .

To tune the general network hyperparameters (Section 4.2), we train a Dense Associative Memory on five tasks and measure the validation accuracy of each task at the end of the respective training period. A grid search over network hyperparameters is performed, with the objective to maximize the minimum validation accuracy of any task – that is, we are seeking a network that can learn tasks as accurately as possible even after training on other tasks. This ensures that the network learns quickly enough to perform well on the first task (overcoming initially random memory vectors) but is also plastic enough to learn new tasks. Note that at this stage we are not tuning for the optimal sequential learning results, only that the network learns quickly and remains plastic. It is likely that previous tasks are quickly forgotten, however new tasks are learned to near completion and are generalized well.

To tune the method hyperparameters (Section 4.3), we again train a Dense Associative Memory on five sequential tasks but now measure the average accuracy at the end of all tasks. Now, instead of tuning the hyperparameters to make a general network to be as plastic as possible, we are tuning parameters to ensure previous tasks are not forgotten, while new tasks are still picked up. This combination of parameter tunings mirrors what we might expect in a practical scenario; starting with a model that is tuned to learn as generally as possible, we apply sequential learning techniques that are tuned to improve sequential learning performance.

## 4.2 Dense Associative Memory Formalization and Hyperparameters

The Dense Associative Memory is an autoassociative memory consisting of a set of memory vectors  $\bar{\zeta}$  that learns a set of items  $\bar{\xi}$  via the gradient descent of the error of the initial item and the relaxed item. To relax a probe state  $\xi$  we update each neuron until all neurons are stable (further updates do not result in change). In contrast to the classical Hopfield

network (Hopfield, 1984), the Dense Associative Memory updates all neuron synchronously. The update for a specific neuron  $\xi_i$  is computed by:

$$\xi_i := \sigma \left( \sum_{\zeta \in \bar{\zeta}} (f_n(\beta \zeta \cdot \xi_{+i}) - f_n(\beta \zeta \cdot \xi_{-i})) \right), \quad (19)$$

where  $\sigma$  is an activation function,  $f_n$  is the interaction function parameterized by the interaction vertex  $n$ ,  $\beta$  is a scaling factor used to adjust the gradient during training, and  $\xi_{+i}, \xi_{-i}$  are the probe state with the  $i^{\text{th}}$  neuron clamped on or off;

$$\begin{aligned} \xi_{+i} &= \begin{cases} +1 & \text{if } i = j \\ \xi_j & \text{if } i \neq j \end{cases}, \\ \xi_{-i} &= \begin{cases} -1 & \text{if } i = j \\ \xi_j & \text{if } i \neq j \end{cases}. \end{aligned}$$

In typical bipolar domain tasks we use  $\sigma = \tanh$  during training so we can take the gradient across the function and  $\sigma = \text{Sign}$  during relaxation, so the probes remain in the space  $\{-1, 1\}^N$ . For classification tasks such as MNIST we use a linear activation on the classification neurons so the results represent logits of the predicted probability distribution for an item. Throughout our experiments we have used the leaky rectified polynomial interaction function

$$f_n(x) = \begin{cases} x^n & \text{if } x > 0 \\ -\epsilon x & \text{otherwise} \end{cases} \quad (20)$$

with  $\epsilon = 10^{-2}$ .

---

**Algorithm 1: Learning Process of the Dense Associative Memory**


---

**Input:** A set of items  $\bar{\xi}$   
**Result:** Trained memory vectors  $\bar{\zeta}$   
**Data:** Number of training epochs  $\text{MaxEpochs}$ , initial learning rate  $\text{lrInit}$ , learning rate decay  $\text{lrDecay}$ , initial temperature  $T_i$ , final temperature  $T_f$ , momentum  $p$ , error exponent  $m$

```

1 Initialize  $\bar{\zeta} \leftarrow \mathcal{N}(\mu = 0, \sigma = 0.1)$ 
2 Initialize MomentumGradient  $\leftarrow 0$ 
3 for  $\text{epoch} \leftarrow 1$  to  $\text{MaxEpochs}$  do
4    $\text{lr} \leftarrow \text{lrInit} \times \text{lrDecay}^{\text{epoch}}$ 
5    $T \leftarrow T_i + (T_f - T_i) \times \frac{\text{epoch}}{\text{MaxEpochs}}$ 
6    $\beta \leftarrow \frac{1}{T}$ 
7   Error  $\leftarrow 0$ 
8   for  $\xi \in \bar{\xi}$  do
9     for  $i \leftarrow 1$  to  $N$  do
10       $\xi_{+i} = \begin{cases} +1 & \text{if } i = j \\ \xi_j & \text{if } i \neq j \end{cases}$ 
11       $\xi_{-i} = \begin{cases} -1 & \text{if } i = j \\ \xi_j & \text{if } i \neq j \end{cases}$ 
12       $\xi'_i \leftarrow \tanh\left(\sum_{\zeta \in \bar{\zeta}} (f_n(\beta\zeta \cdot \xi_{+i}) - f_n(\beta\zeta \cdot \xi_{-i}))\right)$ 
13      Error  $:= \text{Error} + (\xi_i - \xi'_i)^{2m}$ 
14    end
15  end
16  Compute EpochGradient  $\leftarrow \nabla_{\bar{\zeta}} \text{Error}$ 
17  MomentumGradient  $\leftarrow p \times \text{MomentumGradient} + \text{EpochGradient}$ 
18   $\bar{\zeta} := \bar{\zeta} - \text{MomentumGradient} \times \text{lr}$ 
19 end

```

---

Algorithm 1 details the learning process of the Dense Associative Memory (Krotov and Hopfield, 2016). The Dense Associative Memory has numerous hyperparameters, documented in Algorithm 1, that can greatly impact the behavior of the network. Previous research (McAlister, Robins, and Szymanski, 2024a) has shown a small modification to the definition of the network’s relaxation function in Equation 19 (namely, moving  $\beta$  inside the interaction function) results in very stable hyperparameter selection across a wide range of interaction vertices. For this reason we were able to tune the network hyperparameters once on the permuted MNIST dataset and use those parameters again throughout the experiments for consistency. We used a number of memories  $|\bar{\zeta}| = 512$ , a number of training epochs  $\text{MaxEpochs} = 500$ , an initial learning rate  $\text{lrInit} = 8 \times 10^{-2}$ , learning rate decay  $\text{lrDecay} = 0.999$ , momentum  $p = 0.6$ , an initial and final temperature value

$\frac{1}{\beta} = T_i = T_f = 0.95$ , and an error exponent  $m = 1$  throughout our experiments. Krotov and Hopfield (Krotov and Hopfield, 2016; Krotov and Hopfield, 2018) found that increasing the error exponent and temperature difference can improve performance at larger interaction vertices, but we found good performance without altering these values thanks to the modifications made to the network. See Appendix A for the results of our gridsearch over the initial learning rate and temperatures, which demonstrates the stability of hyperparameters across interaction vertex values.

Algorithm 1 is modified slightly in practice – implementing minibatches over the items and clamping memory weights to the interval  $[-1, 1]$  each update. The classification neuron weights are left unclamped, in consistency with other literature.

### 4.3 Sequential Learning Methods Hyperparameters

Each sequential learning method in Section 3 has associated hyperparameters that must also be tuned to maximize sequential learning performance. Instead of fixing the hyperparameters across all interaction vertices as we have done for the more general hyperparameters of the Dense Associative Memory, we will tune the parameters per interaction vertex.

For rehearsal based methods, we varied the proportion of task items added to the rehearsal buffer. We conduct a linear search from a rehearsal proportion of 0.0 to 1.0. For naive rehearsal, this range corresponds to vanilla sequential learning (no sequential learning method) to effectively presenting the tasks non-sequentially. For pseudorehearsal, the lower end of the search again corresponds to no method, but the upper end no longer has a nice interpretation. We can generate as many buffer items as we like, including more than the number of items in the original task. Since we do not require unique generated items, we are likely to generate several repeated items in the buffer, but since the generated items are representative of the network’s attractor space this is not only acceptable, but perhaps preferable to ensure important regions are well sampled. We do not explore beyond a pseudorehearsal proportion of 1.0 as we see a plateau in the performance.

For regularization based methods – L2 Regularization, Elastic Weight Consolidation, Memory Aware Synapses, and Synaptic Intelligence – we must tune the regularization parameter  $\lambda$ . Since the weight importances of each method are not guaranteed to be on the same order of magnitude as one another, we do not expect the values of  $\lambda$  between each method to be comparable. However, the values of  $\lambda$  *within* each method *are* comparable, so if we observe different optimal regularization parameters across interaction vertices that is an interesting result. Again, we perform a search across a wide range of regularization parameters for each method, although this time we employ a log-space search to ensure we explore a wide range of parameters across many orders of magnitude efficiently.

Finally, for the two somewhat unique methods of Gradient Episodic Memories and Averaged Gradient Episodic Memories, we again tune the proportion of data from previous tasks to add to the memory buffer. This allows us to compare the rehearsal methods with

the GEM family of methods. For a specific rehearsal proportion we may find that naive rehearsal results in better average accuracy than GEM or A-GEM, however we must not forget that the GEM family explicitly allows for backwards transfer and more plasticity during learning whereas naive rehearsal is more likely to reinforce the existing memory structures without continued learning on previous tasks, leading to reduced plasticity.

## 5 Experiment Results

### 5.1 Sequential Learning Methods Hyperparameter Tuning

#### 5.1.1 Rehearsal Methods

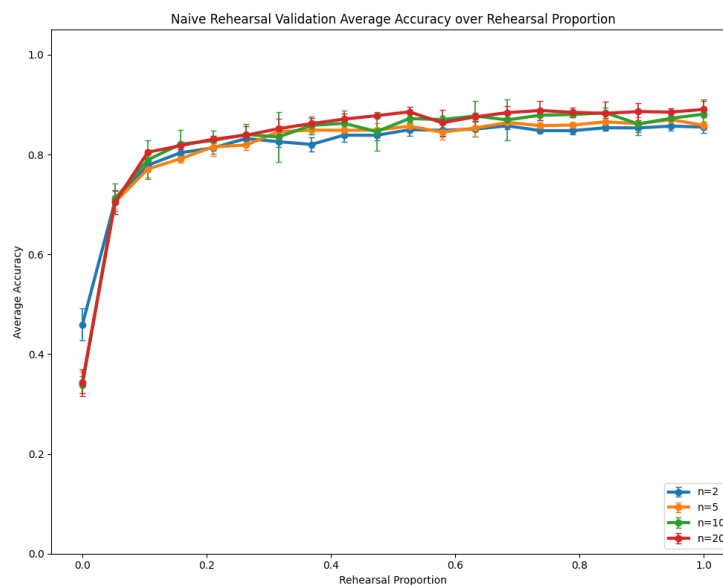


Figure 1: Naive rehearsal hyperparameter search over rehearsal proportion, measuring the average accuracy on the validation data split. A rehearsal proportion of 0.0 corresponds to vanilla learning, while 1.0 corresponds to presenting all previous tasks alongside the new task. A higher average accuracy reflects better performance on sequential learning tasks.

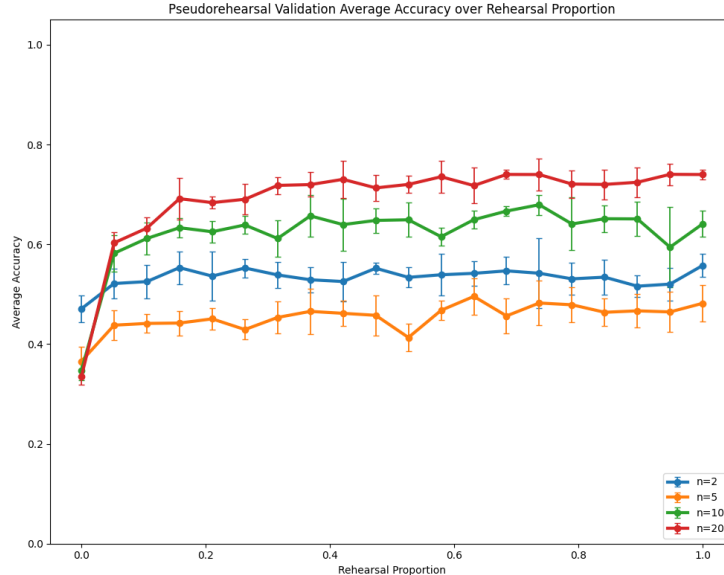


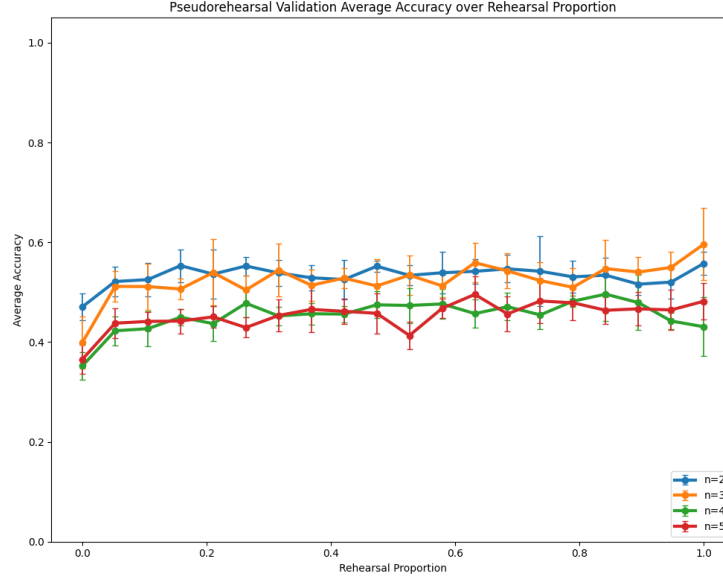
Figure 2: Pseudorehearsal hyperparameter search over rehearsal proportion, measuring the average accuracy on the validation data split. Rehearsal proportion determines the number of pseudoitems generated as a ratio to the number of items in a task. A rehearsal proportion of 0.0 corresponds to vanilla learning. A higher average accuracy reflects better performance on sequential learning tasks.

Our hyperparameter tuning for naive rehearsal, Figure 1, shows a reasonably expected response to the rehearsal proportion. As more items are added to the buffer, the average accuracy increases. This sets a good benchmark for future sequential learning methods, as no method should be able to outperform the simple solution of presenting all tasks at once. Perhaps most interestingly, and unique to naive rehearsal, all interaction vertices appear to perform equally well at non-trivial rehearsal proportions. This indicates that five Permuted MNIST tasks are not overly difficult for this network with a number of memories  $|\bar{\zeta}| = 512$ , no matter the interaction vertex. This is not always true, as we will see with future methods. For a rehearsal proportion of zero,  $n = 2$  seems to outperform  $n > 2$ , which could be due to higher interaction vertices learning new tasks faster and hence forgetting old tasks faster too. A rehearsal proportion of 0.0 also exhibits a very small error, meaning the network is very consistent in sequential learning performance when no additional methods are included (something we also observed in our general hyperparameter tunings, see Appendix A).

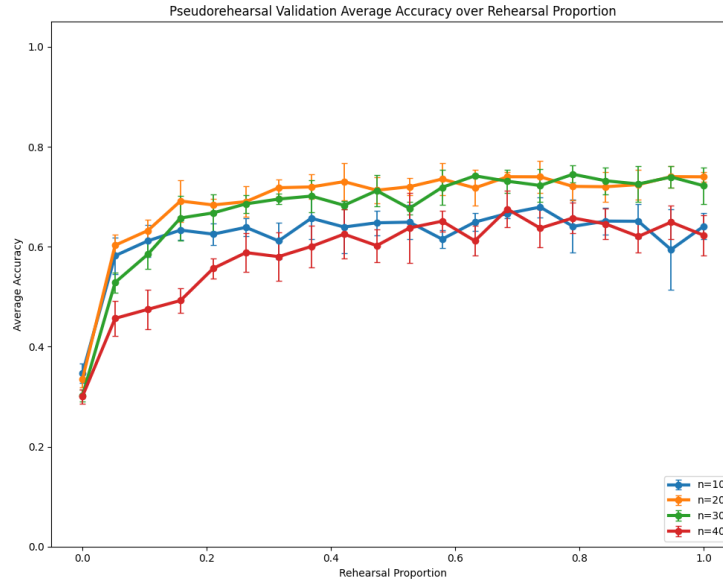
Pseudorehearsal, Figure 2 shows a much more interesting result compared to naive rehearsal. Low interaction vertices,  $n = 2$  and  $n = 5$ , have a reasonably flat response to the rehearsal proportion. We believe this shows that low interaction vertices produce pseudoitems that are not representative of the task data and hence are not useful in preserving previous task when rehearsed. In contrast, higher interaction vertices achieve much higher

validation average accuracy — high interaction vertex networks may generate pseudoitems that are useful in preserving previous task performance due to the feature-to-prototype transition described by Krotov and Hopfield (2016). While we do not quite reach naive rehearsal levels of performance, we do observe very good sequential learning performance for even modest rehearsal proportions. For a rehearsal proportion of 0.0 we find performances that are nearly identical to naive rehearsal using the same proportion, as expected.

We also investigate the behavior of pseudorehearsal for more interaction vertices, since this method offers insight into the recall behavior of the Dense Associative Memory. Notably, we observe a separate behavior transition in the network for low interaction vertices. In Figure 3a we see that pseudoitems generated at  $n \leq 3$  are apparently significantly more useful in preserving previous tasks compared to  $n = 4, 5$  — far below the interaction vertices at which the feature-to-prototype transition occurs. This indicates that there is perhaps more nuance to the network’s behaviors and memory structure than only the feature-to-prototype transition. Unlike the visually striking transition of memory structure, the cause of the performance difference in Figure 3a is much less clear. The pseudoitems generated from each interaction vertices in the Figure are extremely similar, so perhaps the network responds differently rather than the data itself updating. We also study pseudorehearsal for larger interaction vertices, up to  $n = 40$ , with results in Figure 3b. We find that the sequential learning performance plateaus for  $n = 20, 30$  and drops again at  $n = 40$ . This could indicate that large interaction vertices undergo yet another behavior change, and the pseudoitems are somehow less useful for preserving previous task performance, although again there was no obvious difference in the generated pseudoitems. Perhaps the network undergoes another transition and responds differently to same generated data, as with lower interaction vertices. However, we could also be observing a drop in the stability of the network, leading to worse performance due to unstable training.



(a) Small interaction vertices.



(b) Large interaction vertices.

Figure 3: Pseudorehearsal hyperparameter search over rehearsal proportion, measuring the average accuracy on the validation data split. Note the legend in these Figures is different from many others in this Section. Rehearsal proportion determines the number of pseudoitems generated as a ratio to the number of items in a task. A rehearsal proportion of 0.0 corresponds to vanilla learning. A higher average accuracy reflects better performance on sequential learning tasks.

### 5.1.2 GEM and A-GEM

Gradient Episodic Memories and Averaged Gradient Episodic Memories have the same reasonably interpretable hyperparameter space as rehearsal-based methods: how much of the previous task do we store. Although we only require the gradients of the buffer items instead of rehearsing them directly, we are still interested in how the size of the buffer effects the performance of the methods.

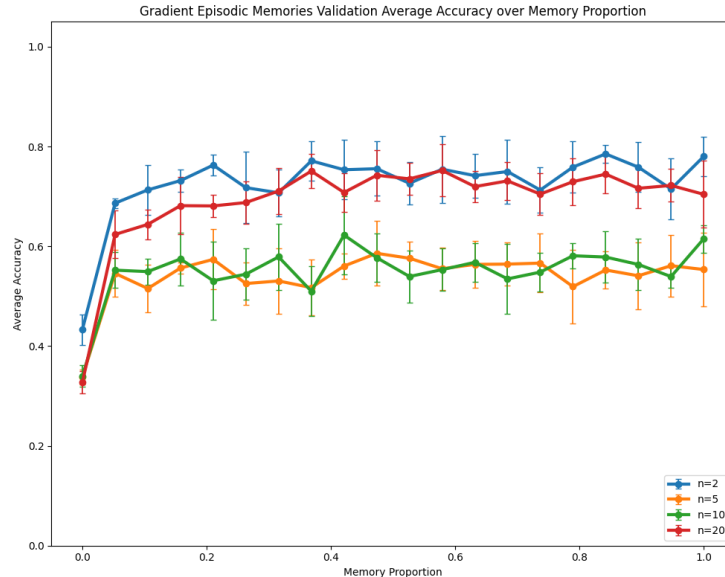


Figure 4: Gradient Episodic Memories hyperparameter search, measuring the average accuracy on the validation data split. A memory proportion of 0.0 corresponds to vanilla learning, while 1.0 checks the gradient across all previous task items. A higher average accuracy reflects better performance on sequential learning tasks.

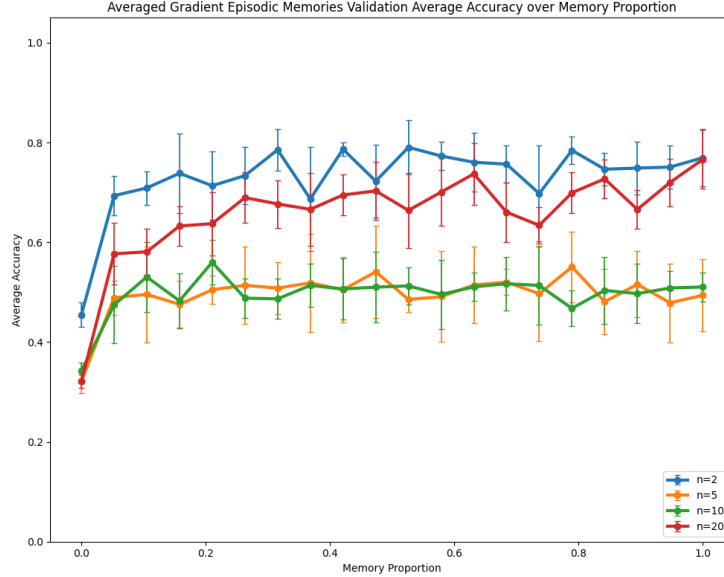


Figure 5: Averaged Gradient Episodic Memories hyperparameter search, measuring the average accuracy on the validation data split. A memory proportion of 0.0 corresponds to vanilla learning, while 1.0 checks the gradient across all previous task items. A higher average accuracy reflects better performance on sequential learning tasks.

In both GEM and A-GEM (Figure 4 and 5 respectively), sequential learning performance peaks for low interaction vertices  $n = 2$  before dropping dramatically, only recovering for high interaction vertices  $n = 20$ . The gulf in performance observed may be due to memory structure changing significantly across these interaction vertices, with the transitory structures being incompatible with the gradient constraints placed by GEM and A-GEM. Certainly it seems that Dense Associative Memories with middling interaction vertices are somehow more sensitive to altering the gradient used for learning than networks with extreme interaction vertices. However, the standard deviations in both methods are much larger than in naive rehearsal or pseudorehearsal, indicating that the Dense Associative Memory is more sensitive to gradient constraints alterations across all interaction vertices. Comparing the two methods, we see there is little difference in performance between GEM and A-GEM. Our findings corroborate Chaudhry et al. (2019) who found that A-GEM — despite relaxing constraints on the theory of GEM — performed just as well on average accuracy. For a memory proportion of 0.0 we find performances that are nearly identical to rehearsal-based methods using the same proportion, as expected as using no items to find a gradient does not constrain learning at all.

### 5.1.3 Regularization-Based Methods

In rehearsal-based methods we have a good understanding of how the rehearsal proportion should impact sequential learning performance and a relatively small space over which to search (0.0 through 1.0), so a grid search was reasonable. In the following regularization-based methods, the regularization hyperparameter  $\lambda$  has a more nuanced impact on performance — too small and the network will forget earlier tasks, too large and the network will not learn new tasks. Furthermore, the search space of  $\lambda$  is much larger, and it is not clear where the optimal region will lie, whereas in rehearsal we could be sure that increasing the rehearsal proportion would improve performance. For these reasons, we have not conducted a grid search over  $\lambda$  but instead use Optuna (Akiba et al., 2019), a hyperparameter optimization library, in conjunction with a Tree-structured Parzen Estimator sampler over the search space. This sampler attempts to estimate the optimal hyperparameter value using a Gaussian Mixture Model, resulting in dense sampling near the optimal region (of interest to us) and sparser sampling far from the optimal region. To estimate the error in the average accuracy across the  $\lambda$  search space, we have used a moving window of size 20 and plot the average and standard deviation (as an error band). This gives us better error estimates close to the optimal region, which is more useful for our analysis. In each of the following methods we have conducted 100 trials for each interaction vertex.

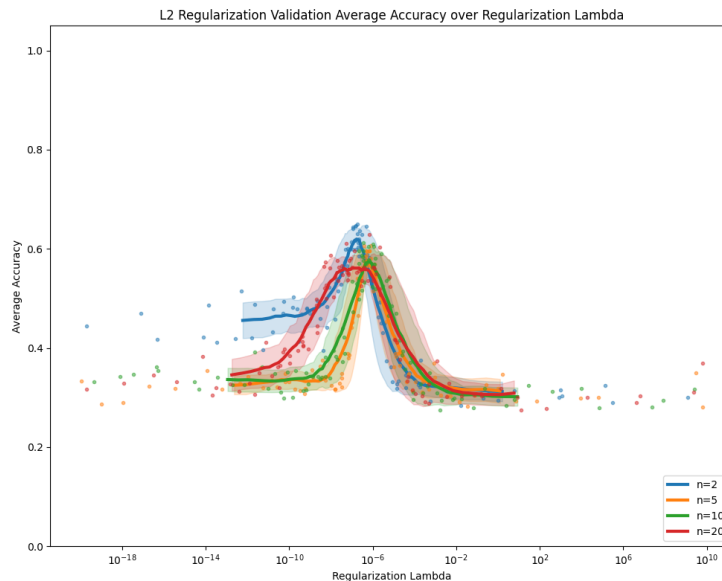
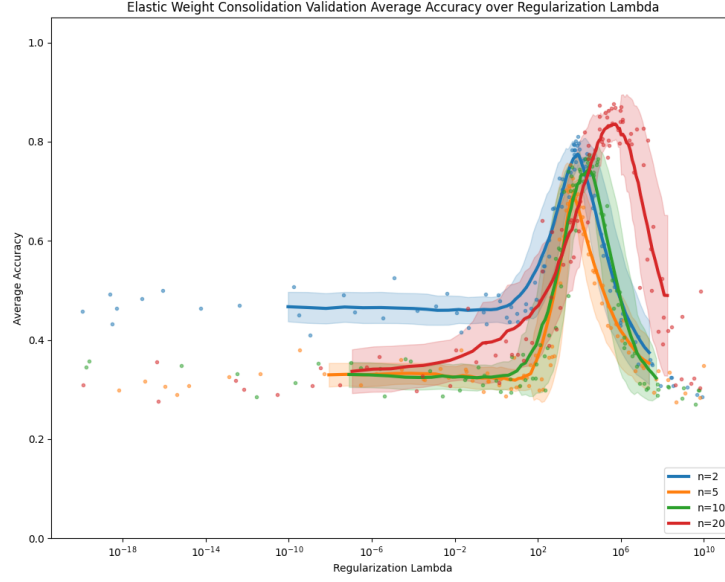


Figure 6: L2 regularization hyperparameter search over regularization hyperparameter  $\lambda$ , measuring the average accuracy on the validation data split. Individual trials are shown as points, and a moving window of size 20 is used to calculate the average (solid lines) and standard deviation (error band). A higher average accuracy reflects better performance on sequential learning tasks.

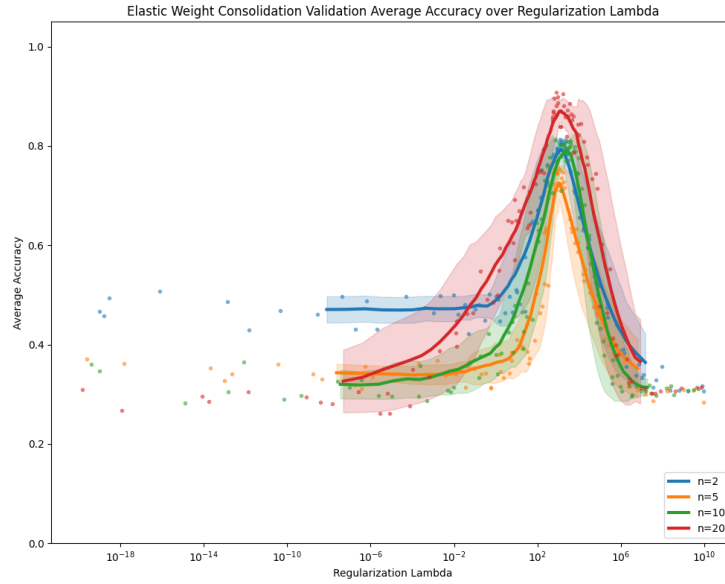
L2 regularization, Figure 6, acts as our baseline for the regularization-based methods, weighting all model parameters equally important. Across all interaction vertices we see a definite peak in average accuracy with tails on either side, as expected. We find that  $n = 2$  gives unique behavior compared to higher interaction vertices; lower-than-optimal values of  $\lambda$  perform much better than higher-than-optimal values, something not reflected in higher interaction vertex results. For very high regularization parameters, the model can learn the first task well but will fail to learn future tasks due to extreme constraints on weight updates, explaining why the average accuracy drops. For very low regularization parameters, the model will forget previous tasks when learning new tasks. In both cases we might expect the model to perform very well only on one task — the first for high regularization parameters and the last task for low regularization parameters — so a symmetrical response to the regularization parameter is expected. The asymmetrical response for  $n = 2$  shows that the Dense Associative Memory is capable of remembering previous tasks better than expected when the regularization parameter is low, perhaps because the network learns “slower” (Krotov and Hopfield, 2016). For higher interaction vertices, the response is much more symmetrical, showing the improved remembering of previous tasks disappears. For  $n = 20$  the response curve has widened somewhat.

The optimal regularization parameter (the peak of the response curve) shifts slightly

as the interaction vertex increases. Unique to L2 regularization, we can interpret this shift directly, as the weight importances are identical and constant. Higher regularization hyperparameters represent the network requiring stronger constraints on previously learned memories in order to retain performance on previous tasks — the learned memories must be more strongly held in place to avoid forgetting. Lower regularization parameters indicate that these constraints can be relatively more relaxed and still retain that performance. In Figure 6 we see that  $n = 2, 20$  both have slightly lower optimal  $\lambda$  values than  $n = 5, 10$ . This, along with our results on GEM and A-GEM, indicate that the memory structures of the transitory interaction vertices behave very differently to the feature or prototype memory structures. In this case, it seems that transitory structures require more constraints to avoid forgetting. We suggest this is due to over-committing of memory vectors. When a new task is introduced, feature-like and prototype-like memories must update a significant amount to contribute strongly to the new task (for extremely unrelated tasks such as Permuted MNIST). Instead, uncommitted memory vectors may receive the bulk of the learning, as they have relatively less distance to update to learn the new task, which in effect preserves the memory vectors associated with previous tasks without requiring explicit constraints. Transitory memory structures may not benefit from this effect — either because they have fewer uncommitted memory vectors at the end of each task, or the relative update distance is smaller as the structures are less organized than features or prototypes.



(a) 2000 items per task.



(b) 10000 items per task.

Figure 7: Elastic Weight Consolidation hyperparameter search over regularization hyperparameter  $\lambda$ , measuring the average accuracy on the validation data split. Individual trials are shown as points, and a moving window of size 20 is used to calculate the average (solid lines) and standard deviation (error band). A higher average accuracy reflects better performance on sequential learning tasks.

Elastic Weight Consolidation, Figure 7a and Figure 7b, shows some similarities to L2 regularization. Again,  $n = 2$  has much higher performance for lower-than-optimal than higher-than-optimal  $\lambda$ , which is not seen for higher interaction vertices. Compared to L2 regularization, the optimal regularization parameter is much higher, which is likely due to the computed weight importances being much smaller than the fixed value used by L2 regularization. Unfortunately, unlike all other regularization methods, we found a significant disparity in the performance of EWC when using the regularization lambda tuned from “small” tasks (Figure 7a) for “large” tasks (Figure 7b). Of particular note, the peak for  $n = 20$  has shifted considerably between the two figures. This is of some interest, even if it makes the network-method combination more difficult to work with in practice. The dependence of the regularization hyperparameter on the amount of data as well as the interaction vertex ( $n < 20$  peaks did not shift between the Figures) could indicate that high interaction vertex networks are more data-hungry than low ones. That is, the prototype-like memory structures are only stabilized strongly for very large amounts of data, and hence the Fisher Information weight importance measure is stronger / larger, explaining the correspondingly lower regularization hyperparameter. The peak performance of EWC increases with the interaction vertex, reaching near naive rehearsal performance for  $n = 20$ . This may indicate that the weight importances are more concentrated in only a few memory vectors, resulting in only some weights being constrained allowing strong constrains (approaching weight freezing) without disrupting plasticity in uncommitted memory vectors. We expect the Fisher Information to approximate the importance of network memories much better than a fixed importance measure, and therefore allow more nuanced constraining of weights than a fixed strategy. This would also explain the improved performance of EWC compared to L2 regularization.

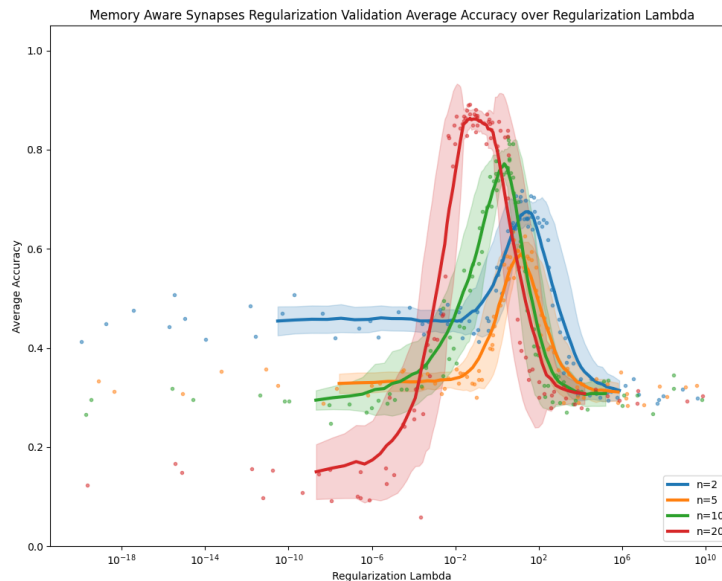


Figure 8: Memory Aware Synapses hyperparameter search over regularization hyperparameter  $\lambda$ , measuring the average accuracy on the validation data split. Individual trials are shown as points, and a moving window of size 20 is used to calculate the average (solid lines) and standard deviation (error band). A higher average accuracy reflects better performance on sequential learning tasks.

Memory Aware Synapses, Figure 8, displays tremendously different behavior compared to Elastic Weight Consolidation. In Memory Aware Synapses, not only do we find the common asymmetrical response curve for  $n = 2$  but also an asymmetrical response for  $n = 20$ , where lower-than-optimal  $\lambda$  values produce terrifically poor performances. As a tradeoff for the sensitivity, it seems that Memory Aware Synapses with a high interaction vertex results in some of the best performances we have observed so far, rivaling even naive rehearsal. There is a consistent shift to smaller optimal regularization parameters as the interaction vertex increases. The consistency of the shift is unique to Memory Aware Synapses, as even Elastic Weight Consolidation with a small task size (Figure 7a) demonstrated a shift for only  $n = 20$ , and L2 regularization had more erratic shifts. Perhaps this indicates that the computed importances are of an increasing magnitude as the interaction vertex increases, or that the “concentration” of weight importance increases to give rise to a consistent left-ward shift in  $\lambda$ . Memory Aware Synapses uses a Taylor expansion across the network outputs to compute the weight importances; for high interaction vertices we would expect the gradients in this expansion to increase, increasing the magnitude of the weight importance measures, offering a potential mechanism for the shift towards smaller regularization parameters. MAS is consistent with L2 regularization and EWC in that higher interaction vertices improve peak average accuracy.

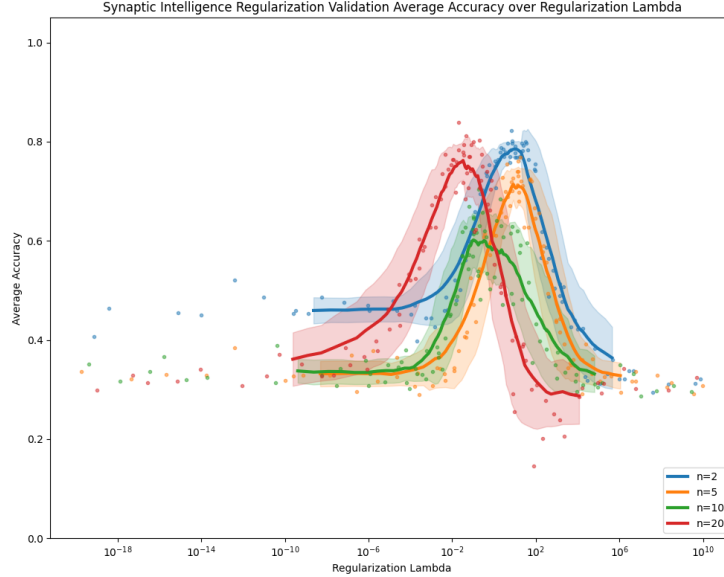


Figure 9: Synaptic Intelligence hyperparameter search over regularization hyperparameter  $\lambda$ , measuring the average accuracy on the validation data split. Individual trials are shown as points, and a moving window of size 20 is used to calculate the average (solid lines) and standard deviation (error band). A higher average accuracy reflects better performance on sequential learning tasks.

Synaptic Intelligence, Figure 9 demonstrates some of the now familiar behaviors seen in both L2 regularization and Elastic Weight Consolidation. The  $n = 2$  average accuracy over  $\lambda$  demonstrates an asymmetrical curve while higher interaction vertices are more symmetrical. However, Synaptic Intelligence displays some decidedly different behavior compared to the above methods. The lowest interaction vertex network now performs better than other networks, although the  $n = 20$  network approaches the  $n = 2$  in terms of performance. This may suggest that Synaptic Intelligence interacts well with feature-like memories — unlike Elastic Weight Consolidation and Memory Aware Synapses. Again, the transitory networks seem to perform particularly poorly. As in Memory Aware Synapses, the optimal regularization parameter decreases for  $n = 20$ , which could be due to a smaller weight importance magnitude. Synaptic Intelligence includes the total weight drift over a task, which could be drastically changed by the interaction vertex. For example, altering a feature-like memory on one task to a feature-like memory on a second task may result in a smaller drift than altering a prototype-like memory on one task to a prototype-like memory on another, even for tasks that are extremely unrelated such as Permuted MNIST. It would be interesting to see if this behavior also arose using tasks that are more related to one another, such as Rotated MNIST. The differences between L2 Regularization and Elastic Weight Consolidation compared to Memory Aware Synapses and Synaptic Intelligence

may also be caused by the slightly different regularization terms — the former add a new loss term per task, while the latter add only a single term that is updated with each task. Aggregating all previous task constraints into a single term may somehow result in decreasing optimal regularization parameters with increasing interaction vertices, although the mechanism for this is not obvious if it exists at all. Testing more regularization-based sequential learning methods may provide more insight.

## 5.2 Tuned Sequential Learning Methods

Now we have tuned the Dense Associative Memory and all sequential learning methods we can finally compare the peak performance of each method to one another. For rehearsal-based methods, GEM, and A-GEM, we investigate several values of the rehearsal / memory proportion. For the regularization-based methods, we use regularization  $\lambda$  as shown in Table 1. We repeat the five Permuted MNIST task sequential learning experiment ten times, aggregating the results in Table 2.

	$n = 2$	$n = 5$	$n = 10$	$n = 20$
L2 Regularization	$1.7 \times 10^{-7}$	$5.4 \times 10^{-7}$	$7.5 \times 10^{-7}$	$2.2 \times 10^{-7}$
Elastic Weight Consolidation	$1.3 \times 10^3$	$1.1 \times 10^3$	$2.3 \times 10^3$	$1.4 \times 10^3$
Memory Aware Synapses	$3.2 \times 10^1$	$1.5 \times 10^1$	$2.2 \times 10^0$	$5.1 \times 10^{-2}$
Synaptic Intelligence	$9.5 \times 10^0$	$8.5 \times 10^0$	$1.0 \times 10^{-1}$	$3.3 \times 10^{-2}$

Table 1: Selection of regularization hyperparameter  $\lambda$  across interaction vertices and sequential learning method.

	$n = 2$	$n = 5$	$n = 10$	$n = 20$
Vanilla	$0.431 \pm 0.027$	$0.325 \pm 0.012$	$0.325 \pm 0.014$	$0.316 \pm 0.004$
Rehearsal Methods - Memory Proportion of 0.05				
Rehearsal	$0.834 \pm 0.004$	$0.843 \pm 0.005$	$0.871 \pm 0.007$	$0.869 \pm 0.010$
Pseudorehearsal	$0.483 \pm 0.030$	$0.436 \pm 0.020$	$0.534 \pm 0.021$	$0.694 \pm 0.015$
GEM	$0.743 \pm 0.019$	$0.607 \pm 0.028$	$0.614 \pm 0.033$	$0.789 \pm 0.025$
A-GEM	$0.746 \pm 0.020$	$0.568 \pm 0.029$	$0.585 \pm 0.034$	$0.802 \pm 0.047$
Rehearsal Methods - Memory Proportion of 0.5				
Rehearsal	$0.880 \pm 0.004$	$0.895 \pm 0.004$	$0.912 \pm 0.011$	$0.904 \pm 0.013$
Pseudorehearsal	$0.452 \pm 0.035$	$0.434 \pm 0.036$	$0.589 \pm 0.042$	$0.787 \pm 0.026$
GEM	$0.768 \pm 0.015$	$0.610 \pm 0.029$	$0.602 \pm 0.032$	$0.854 \pm 0.017$
A-GEM	$0.757 \pm 0.019$	$0.585 \pm 0.028$	$0.601 \pm 0.024$	$0.848 \pm 0.036$
Regularization Methods				
L2 Regularization	$0.685 \pm 0.019$	$0.597 \pm 0.015$	$0.554 \pm 0.025$	$0.599 \pm 0.035$
Elastic Weight Consolidation	$0.711 \pm 0.024$	$0.553 \pm 0.017$	$0.554 \pm 0.051$	$0.838 \pm 0.052$
Memory Aware Synapses	$0.775 \pm 0.020$	$0.650 \pm 0.020$	$0.841 \pm 0.027$	$0.833 \pm 0.021$
Synaptic Intelligence	$0.770 \pm 0.010$	$0.724 \pm 0.015$	$0.642 \pm 0.061$	$0.803 \pm 0.032$

Table 2: Average Accuracy over five Permuted MNIST tasks using different sequential learning methods. Vanilla indicates training with no additional sequential learning method. Methods with a number note the memory proportion used, either as rehearsal items or for gradient calculations. Results are aggregated over ten trials each, and the standard deviation is reported after the  $\pm$ .

For the rehearsal and GEM family of methods, we only investigate two memory proportions, 0.05 and 0.50, as our hyperparameter searches found a steep initial response followed by a long plateau. See Figures 1 and 2 for rehearsal-based methods and Figures 4 and 5 for GEM family methods. That is, a small memory proportion gives substantial benefits over zero memory proportion (vanilla learning) and there is little improvement beyond a modest memory proportion.

We find results that are largely in agreement with the hyperparameter tunings from Section 4.3. The notable exception, of course, being Elastic Weight Consolidation which required tuning with tasks of a larger number of items, so in this sense Elastic Weight Consolidation is at a slight advantage to the other methods. This is important to note, since we found that Elastic Weight Consolidation to be the best regularization-based sequential learning method for  $n = 20$ . Memory Aware Synapses and Synaptic Intelligence have a significantly better performance for  $n = 2$ , and remain more consistent than Elastic Weight Consolidation across the transitory interaction vertices  $n = 5, 10$ . The rehearsal-based methods have an unsurprising winner — naive rehearsal is the best sequential learning method from all presented. However, pseudorehearsal shows its massively improved performance at higher interaction vertices, shifting from near vanilla performance at  $n = 2, 5$

to respectable performances at  $n = 20$ . GEM and A-GEM are notable not only for their bimodal performance peaks for both memory proportions tested, but also their significantly larger standard deviations compared to the other methods. Vanilla sequential learning (with no sequential learning method) is presented for a comparison. Note that for vanilla sequential learning, the average accuracy decreases with the interaction vertex even down to  $n = 20$ , meaning the improved performance seen at higher interaction vertices for some methods (e.g. pseudorehearsal, GEM, A-GEM) is even more impressive as the baseline is significantly lower than the low interaction vertex network.

## 6 Conclusions

We have investigated the Dense Associative Memory in the context of sequential learning. We believe the application of this network in a sequential learning environment is novel, and gives some insight into the behavior of this associative memory architecture. Our studies include rehearsal-based (naive rehearsal, pseudorehearsal), gradient-based (Gradient Episodic Memories, Averaged Gradient Episodic Memories) and regularization-based (L2 Regularization, Elastic Weight Consolidation, Memory Aware Synapses, Synaptic Intelligence) sequential learning methods. Our studies shed light on several aspects of the Dense Associative Memory; the performance of the network in sequential learning tasks, the most effective sequential learning method as the interaction vertex varies, and the properties of the network more broadly.

We found that the Dense Associative Memory responds as expected to rehearsal-based methods; increasing the average accuracy of a series of tasks as more of the previous tasks are rehearsed. Of particular note was pseudorehearsal, which improved dramatically at high interaction vertices, which we attribute to the generation of representative pseudoitems thanks to prototype-like memory structures. Gradient-based methods (GEM, A-GEM) were very effective at extreme interaction vertices but much less effective at transitory values, and also produced much more unstable learning behaviors, perhaps indicating the Dense Associative Memory is very sensitive to gradient alterations during the learning process.

Regularization-based methods gave some understanding of weight importances in the Dense Associative Memory. From a sequential learning perspective, the network behaves typically in that constraining the weights retains performance on previous tasks, even for naive constraints such as L2 regularization. We discovered that the regularization hyperparameter in Elastic Weight Consolidation was sensitive to the amount of data used per task, particularly for higher interaction vertices, which may indicate that the prototype memory structures of high interaction vertex networks require increasing amounts of data to stabilize (at least, in a way that the Fisher Information can attribute importances to). We found that Memory Aware Synapses and Synaptic Intelligence performed very well for transitory interaction vertices where other methods struggled, and regularization-based

methods worked as well as rehearsal-based methods in most cases.

Our findings seem to indicate that the Dense Associative Memory operates reasonably typically in a sequential learning environment, and existing sequential learning methods can be applied directly. Higher interaction vertex networks improve their performance much more than low interaction vertex networks, although both are equally capable of learning the Permuted MNIST tasks we tested. Transitory interaction vertex networks tend to have the worst performance, although some sequential learning methods work particularly well. It seems that while a higher interaction vertex gives improved capacity, performance, and representations of task data, this comes at the cost of requiring larger datasets and a more temperamental network.

## References

- Aich, Abhishek (May 2021). *Elastic Weight Consolidation (EWC): Nuts and Bolts*. arXiv:2105.04093 [cs, stat]. DOI: 10.48550/arXiv.2105.04093.
- Akiba, Takuya et al. (July 2019). “Optuna: A Next-generation Hyperparameter Optimization Framework”. In: *Proceedings of the 25th ACM SIGKDD International Conference on Knowledge Discovery & Data Mining*. KDD ’19. New York, NY, USA: Association for Computing Machinery, pp. 2623–2631. ISBN: 978-1-4503-6201-6. DOI: 10.1145/3292500.3330701. URL: <https://dl.acm.org/doi/10.1145/3292500.3330701> (visited on 09/09/2024).
- Aljundi, Rahaf et al. (Oct. 2018). *Memory Aware Synapses: Learning what (not) to forget*. arXiv:1711.09601 [cs, stat]. DOI: 10.48550/arXiv.1711.09601.
- Amit, Daniel J. (Jan. 1994). “11 - Psychology, Neurobiology and Modeling: The Science of Hebbian Reverberations”. In: *Neural Modeling and Neural Networks*. Ed. by F. Ventriglia. Pergamon Studies in Neuroscience. Amsterdam: Pergamon, pp. 251–281. DOI: 10.1016/B978-0-08-042277-0.50016-2.
- Amit, Daniel J., Hanoch Gutfreund, and H. Sompolinsky (Aug. 1985a). “Spin-glass models of neural networks”. In: *Physical Review A* 32.2. Publisher: American Physical Society, pp. 1007–1018. DOI: 10.1103/PhysRevA.32.1007.
- (Sept. 1985b). “Storing Infinite Numbers of Patterns in a Spin-Glass Model of Neural Networks”. In: *Physical Review Letters* 55.14. Publisher: American Physical Society, pp. 1530–1533. DOI: 10.1103/PhysRevLett.55.1530.
- Amit, Daniel J, Hanoch Gutfreund, and H Sompolinsky (Jan. 1987). “Statistical mechanics of neural networks near saturation”. In: *Annals of Physics* 173.1, pp. 30–67. ISSN: 0003-4916. DOI: 10.1016/0003-4916(87)90092-3.
- Atkinson, Craig et al. (Mar. 2021). “Pseudo-Rehearsal: Achieving Deep Reinforcement Learning without Catastrophic Forgetting”. en. In: *Neurocomputing* 428. arXiv:1812.02464 [cs], pp. 291–307. ISSN: 09252312. DOI: 10.1016/j.neucom.2020.11.050. URL: <http://arxiv.org/abs/1812.02464> (visited on 08/22/2024).

- Bovier, Anton and Beat Niederhauser (Sept. 2001). “The spin-glass phase-transition in the Hopfield model with p-spin interactions”. In: *Advances in Theoretical and Mathematical Physics* 5, pp. 1001–1046. DOI: 10.4310/ATMP.2001.v5.n6.a2.
- Burgess, Neil, J. L. Shapiro, and M. A. Moore (Jan. 1991). “Neural network models of list learning”. EN. In: *Network: Computation in Neural Systems*. Publisher: Taylor & Francis. DOI: 10.1088/0954-898X\_2\_4\_005.
- Caccia, Massimo et al. (Jan. 2021). *Online Fast Adaptation and Knowledge Accumulation: a New Approach to Continual Learning*. en. arXiv:2003.05856 [cs].
- Chaudhry, Arslan et al. (Dec. 2018). *Efficient Lifelong Learning with A-GEM*. en. URL: <https://arxiv.org/abs/1812.00420v2> (visited on 07/31/2024).
- Chaudhry, Arslan et al. (June 2019). *On Tiny Episodic Memories in Continual Learning*. arXiv:1902.10486 [cs, stat]. DOI: 10.48550/arXiv.1902.10486.
- Ceciu, Denisa, Mathias Bode, and Radwa Khalil (Mar. 2024). “Reconstructing creative thoughts: Hopfield neural networks”. In: *Neurocomputing* 575, p. 127324. ISSN: 0925-2312. DOI: 10.1016/j.neucom.2024.127324.
- Demircigil, Mete et al. (July 2017). “On a Model of Associative Memory with Huge Storage Capacity”. en. In: *Journal of Statistical Physics* 168.2, pp. 288–299. ISSN: 0022-4715, 1572-9613. DOI: 10.1007/s10955-017-1806-y.
- Douillard, Arthur et al. (Aug. 2022). *DyTox: Transformers for Continual Learning with Dynamic TOken eXpansion*. arXiv:2111.11326 [cs]. DOI: 10.48550/arXiv.2111.11326.
- Frean, Marcus (Nov. 1992). “A ”Thermal” Perceptron Learning Rule”. In: *Neural Computation* 4.6, pp. 946–957. ISSN: 0899-7667. DOI: 10.1162/neco.1992.4.6.946. URL: <https://doi.org/10.1162/neco.1992.4.6.946> (visited on 09/09/2024).
- Goodfellow, Ian J. et al. (Mar. 2015). *An Empirical Investigation of Catastrophic Forgetting in Gradient-Based Neural Networks*. en. arXiv:1312.6211 [cs, stat]. (Visited on 08/20/2024).
- Hebb, D. O. (1949). *The organization of behavior; a neuropsychological theory*. The organization of behavior; a neuropsychological theory. Pages: xix, 335. Oxford, England: Wiley.
- Hertz, John A. (1991). *Introduction To The Theory Of Neural Computation*. Boca Raton: CRC Press. ISBN: 978-0-429-49966-1. DOI: 10.1201/9780429499661.
- Hopfield, J J (Apr. 1982). “Neural networks and physical systems with emergent collective computational abilities.” In: *Proceedings of the National Academy of Sciences of the United States of America* 79.8, pp. 2554–2558. ISSN: 0027-8424. (Visited on 02/22/2024).
- Hopfield, J. J. (1984). “Neurons with Graded Response Have Collective Computational Properties like Those of Two-State Neurons”. In: *Proceedings of the National Academy of Sciences of the United States of America* 81.10. Publisher: National Academy of Sciences, pp. 3088–3092. ISSN: 0027-8424.
- (Mar. 1999). “Brain, neural networks, and computation”. In: *Reviews of Modern Physics* 71.2. Publisher: American Physical Society, S431–S437. DOI: 10.1103/RevModPhys.71.S431.

- Houlsby, Neil et al. (May 2019). “Parameter-Efficient Transfer Learning for NLP”. en. In: *Proceedings of the 36th International Conference on Machine Learning*. ISSN: 2640-3498. PMLR, pp. 2790–2799. (Visited on 08/20/2024).
- Kirkpatrick, James et al. (Mar. 2017). “Overcoming catastrophic forgetting in neural networks”. en. In: *Proceedings of the National Academy of Sciences* 114.13. arXiv:1612.00796 [cs, stat], pp. 3521–3526. ISSN: 0027-8424, 1091-6490. DOI: 10.1073/pnas.1611835114.
- Kirkpatrick, Scott and David Sherrington (June 1978). “Infinite-ranged models of spin-glasses”. In: *Physical Review B* 17.11. Publisher: American Physical Society, pp. 4384–4403. DOI: 10.1103/PhysRevB.17.4384.
- Kohonen, T. (Dec. 1978). *Associative Memory: A System-Theoretical Approach*. en. Google Books-ID: 7wPtCAAQBAJ. Springer Science & Business Media. ISBN: 978-3-642-96384-1.
- Kohonen, Teuvo (Apr. 1972). “Correlation Matrix Memories”. en. In: *IEEE Transactions on Computers* C-21.4, pp. 353–359. ISSN: 0018-9340. DOI: 10.1109/TC.1972.5008975.
- Krizhevsky, Alex and Geoffrey Hinton (2009). “Learning Multiple Layers of Features from Tiny Images”. en. In: *University of Toronto, ON, Canada*.
- Krizhevsky, Alex, Ilya Sutskever, and Geoffrey E Hinton (2012). “ImageNet Classification with Deep Convolutional Neural Networks”. In: *Advances in Neural Information Processing Systems*. Vol. 25. Curran Associates, Inc. (Visited on 08/20/2024).
- Krotov, Dmitry and John Hopfield (Dec. 2018). “Dense Associative Memory Is Robust to Adversarial Inputs”. In: *Neural Computation* 30.12, pp. 3151–3167. ISSN: 0899-7667. DOI: 10.1162/neco\_a\_01143.
- Krotov, Dmitry and John J. Hopfield (Sept. 2016). *Dense Associative Memory for Pattern Recognition*. arXiv:1606.01164 [cond-mat, q-bio, stat]. DOI: 10.48550/arXiv.1606.01164.
- Lampert, Christoph H., Hannes Nickisch, and Stefan Harmeling (June 2009). “Learning to detect unseen object classes by between-class attribute transfer”. In: *2009 IEEE Conference on Computer Vision and Pattern Recognition*. Conference Name: 2009 IEEE Computer Society Conference on Computer Vision and Pattern Recognition Workshops (CVPR Workshops) ISBN: 9781424439928 Place: Miami, FL Publisher: IEEE, pp. 951–958. DOI: 10.1109/CVPR.2009.5206594. (Visited on 08/20/2024).
- LeCun, Yann, Corrina Cortes, and Christopher Burges (1998). *MNIST handwritten digit database, Yann LeCun, Corinna Cortes and Chris Burges*.
- Lewis, David et al. (Apr. 2004). “RCV1: A New Benchmark Collection for Text Categorization Research.” In: *Journal of Machine Learning Research* 5, pp. 361–397.
- Li, Duo et al. (Jan. 2022). *Technical Report for ICCV 2021 Challenge SSLAD-Track3B: Transformers Are Better Continual Learners*. arXiv:2201.04924 [cs]. DOI: 10.48550/arXiv.2201.04924. (Visited on 08/20/2024).
- Lopez-Paz, David and Marc’Aurelio Ranzato (Sept. 2022). *Gradient Episodic Memory for Continual Learning*. arXiv:1706.08840 [cs]. DOI: 10.48550/arXiv.1706.08840.

- Lund, F. H. (1925). “The psychology of belief”. In: *The Journal of Abnormal and Social Psychology* 20.1. Place: US Publisher: American Psychological Association, pp. 63–81; 174–195. ISSN: 0096-851X. DOI: 10.1037/h0076047.
- Maass, Wolfgang and Thomas Natschl ger (Jan. 1997). “Networks of spiking neurons can emulate arbitrary Hopfield nets in temporal coding”. In: *Network: Computation in Neural Systems* 8.4. Publisher: Taylor & Francis .eprint: [https://doi.org/10.1088/0954-898X\\_8\\_4\\_002](https://doi.org/10.1088/0954-898X_8_4_002), pp. 355–371. ISSN: 0954-898X. DOI: 10.1088/0954-898X\_8\_4\_002.
- McAlister, Hayden, Anthony Robins, and Lech Szymanski (July 2024a). *Improved Robustness and Hyperparameter Selection in Modern Hopfield Networks*. arXiv:2407.08742 [cs]. DOI: 10.48550/arXiv.2407.08742. (Visited on 08/20/2024).
- (May 2024b). *Prototype Analysis in Hopfield Networks with Hebbian Learning*. arXiv:2407.03342 [cond-mat]. DOI: 10.48550/arXiv.2407.03342.
- McEliece, R. et al. (July 1987). “The capacity of the Hopfield associative memory”. In: *IEEE Transactions on Information Theory* 33.4. Conference Name: IEEE Transactions on Information Theory, pp. 461–482. ISSN: 1557-9654. DOI: 10.1109/TIT.1987.1057328.
- Nadal, J. P. et al. (May 1986). “Networks of Formal Neurons and Memory Palimpsests”. en. In: *Europhysics Letters* 1.10, p. 535. ISSN: 0295-5075. DOI: 10.1209/0295-5075/1/10/008.
- Pascanu, Razvan and Yoshua Bengio (Feb. 2014). *Revisiting Natural Gradient for Deep Networks*. arXiv:1301.3584 [cs]. DOI: 10.48550/arXiv.1301.3584. URL: <http://arxiv.org/abs/1301.3584> (visited on 08/28/2024).
- Personnaz, L. et al. (May 1986). “A biologically constrained learning mechanism in networks of formal neurons”. en. In: *Journal of Statistical Physics* 43.3, pp. 411–422. ISSN: 1572-9613. DOI: 10.1007/BF01020645. URL: <https://doi.org/10.1007/BF01020645> (visited on 09/09/2024).
- Ramsauer, Hubert et al. (Apr. 2021). *Hopfield Networks is All You Need*. en. arXiv:2008.02217 [cs, stat].
- Robins, Anthony (Nov. 1993). “Catastrophic forgetting in neural networks: the role of rehearsal mechanisms”. In: *Proceedings 1993 The First New Zealand International Two-Stream Conference on Artificial Neural Networks and Expert Systems*, pp. 65–68. DOI: 10.1109/ANNES.1993.323080.
- (June 1995). “Catastrophic Forgetting, Rehearsal and Pseudorehearsal”. EN. In: *Connection Science*. Publisher: Taylor & Francis Group. DOI: 10.1080/09540099550039318.
- Robins, Anthony and Simon McCallum (June 1998). “Catastrophic Forgetting and the Pseudorehearsal Solution in Hopfield-type Networks”. EN. In: *Connection Science*. Publisher: Taylor & Francis Group. DOI: 10.1080/095400998116530.
- Robins, Anthony V. and Simon J. R. McCallum (Apr. 2004). “A robust method for distinguishing between learned and spurious attractors”. eng. In: *Neural Networks: The Official Journal of the International Neural Network Society* 17.3, pp. 313–326. ISSN: 0893-6080. DOI: 10.1016/j.neunet.2003.11.007.

- Shiffrin, R. M. and R. C. Atkinson (1969). “Storage and retrieval processes in long-term memory”. In: *Psychological Review* 76.2. Place: US Publisher: American Psychological Association, pp. 179–193. ISSN: 1939-1471. DOI: 10.1037/h0027277.
- Silver, Daniel L., Geoffrey Mason, and Lubna Eljabu (2015). “Consolidation Using Sweep Task Rehearsal: Overcoming the Stability-Plasticity Problem”. en. In: *Advances in Artificial Intelligence*. Ed. by Denilson Barbosa and Evangelos Milios. Vol. 9091. Series Title: Lecture Notes in Computer Science. Cham: Springer International Publishing, pp. 307–322. ISBN: 978-3-319-18355-8 978-3-319-18356-5. DOI: 10.1007/978-3-319-18356-5\_27. URL: [https://link.springer.com/10.1007/978-3-319-18356-5\\_27](https://link.springer.com/10.1007/978-3-319-18356-5_27) (visited on 08/22/2024).
- Snow, Mallory (Dec. 2022). “Biological Plausibility in Modern Hopfield Networks”. en. In: Publisher: University of Waterloo.
- Steinbuch, K. and U. A. W. Piske (Dec. 1963). “Learning matrices and their applications”. In: *IEEE Transactions on Electronic Computers* EC-12.6. Conference Name: IEEE Transactions on Electronic Computers. ISSN: 0367-7508. DOI: 10.1109/PGEC.1963.263588.
- Steinbuch, Karl (Feb. 1965). “Adaptive networks using learning matrices”. en. In: *Kybernetik* 2.4, pp. 148–152. ISSN: 1432-0770. DOI: 10.1007/BF00272311.
- Stork (June 1989). “Is backpropagation biologically plausible?” In: *International 1989 Joint Conference on Neural Networks*, 241–246 vol.2. DOI: 10.1109/IJCNN.1989.118705.
- Storkey, Amos (1997). “Increasing the capacity of a hopfield network without sacrificing functionality”. en. In: *Artificial Neural Networks — ICANN’97*. Ed. by Wulfram Gerstner et al. Lecture Notes in Computer Science. Berlin, Heidelberg: Springer, pp. 451–456. ISBN: 978-3-540-69620-9. DOI: 10.1007/BFb0020196.
- Toulouse, G., S. Dehaene, and J. P. Changeux (Mar. 1986). “Spin glass model of learning by selection”. eng. In: *Proceedings of the National Academy of Sciences of the United States of America* 83.6, pp. 1695–1698. ISSN: 0027-8424. DOI: 10.1073/pnas.83.6.1695.
- Tsodyks, Misha (1999). “Attractor neural network models of spatial maps in hippocampus”. fr. In: *Hippocampus* 9.4, pp. 481–489. ISSN: 1098-1063. DOI: 10.1002/(SICI)1098-1063(1999)9:4<481::AID-HIP014>3.0.CO;2-S.
- Vaswani, Ashish et al. (Dec. 2017). “Attention is all you need”. In: NIPS’17, pp. 6000–6010.
- Welinder, Peter et al. (Sept. 2010). “Caltech-UCSD Birds 200”. In.
- Widrow, Bernard and Marcian E. Hoff (1960). “Adaptive switching circuits”. en. In: DOI: 10.7551/mitpress/4943.003.0012.
- Yang, Pengcheng et al. (June 2018). “SGM: Sequence Generation Model for Multi-label Classification”. In: (visited on 08/20/2024).
- Zenke, Friedemann, Ben Poole, and Surya Ganguli (July 2017). “Continual Learning Through Synaptic Intelligence”. en. In: *Proceedings of the 34th International Conference on Machine Learning*. ISSN: 2640-3498. PMLR, pp. 3987–3995.
- Zubiaga, Arkaitz (Feb. 2012). *Enhancing Navigation on Wikipedia with Social Tags*. arXiv:1202.5469 [cs]. DOI: 10.48550/arXiv.1202.5469. (Visited on 08/20/2024).

## A General Dense Associative Memory Hyperparameter Search

We conducted a hyperparameter search over the general network hyperparameters. Our aim is to find the combination of hyperparameters that maximizes the minimum accuracy on these tasks. This ensures our network can not only learn the first task well (overcoming initialization) but also remain plastic enough to learn subsequent tasks. We present a select few of these gridsearches that performed best, searching over the initial learning rate and the temperature. We repeated these experiments to tune the learning rate decay and momentum values, although the results are excluded for brevity. Note that the optimal regions in the searches below do not move considerably as we increase the interaction vertex, something attributed to modifications to the Dense Associative Memory (McAlister, Robins, and Szymanski, 2024a). We also include the average accuracy over the same gridsearch for completeness. We determined the optimal general network hyperparameters to be a number of memories  $|\bar{\zeta}| = 512$ , a number of training epochs  $\text{MaxEpochs} = 500$ , an initial learning rate  $\text{lrInit} = 1 \times 10^{-1}$ , learning rate decay  $\text{lrDecay} = 0.999$ , momentum  $p = 0.6$ , an initial and final temperature value  $\frac{1}{\beta} = T_i = T_f = 0.875$ , and an error exponent  $m = 1$ .

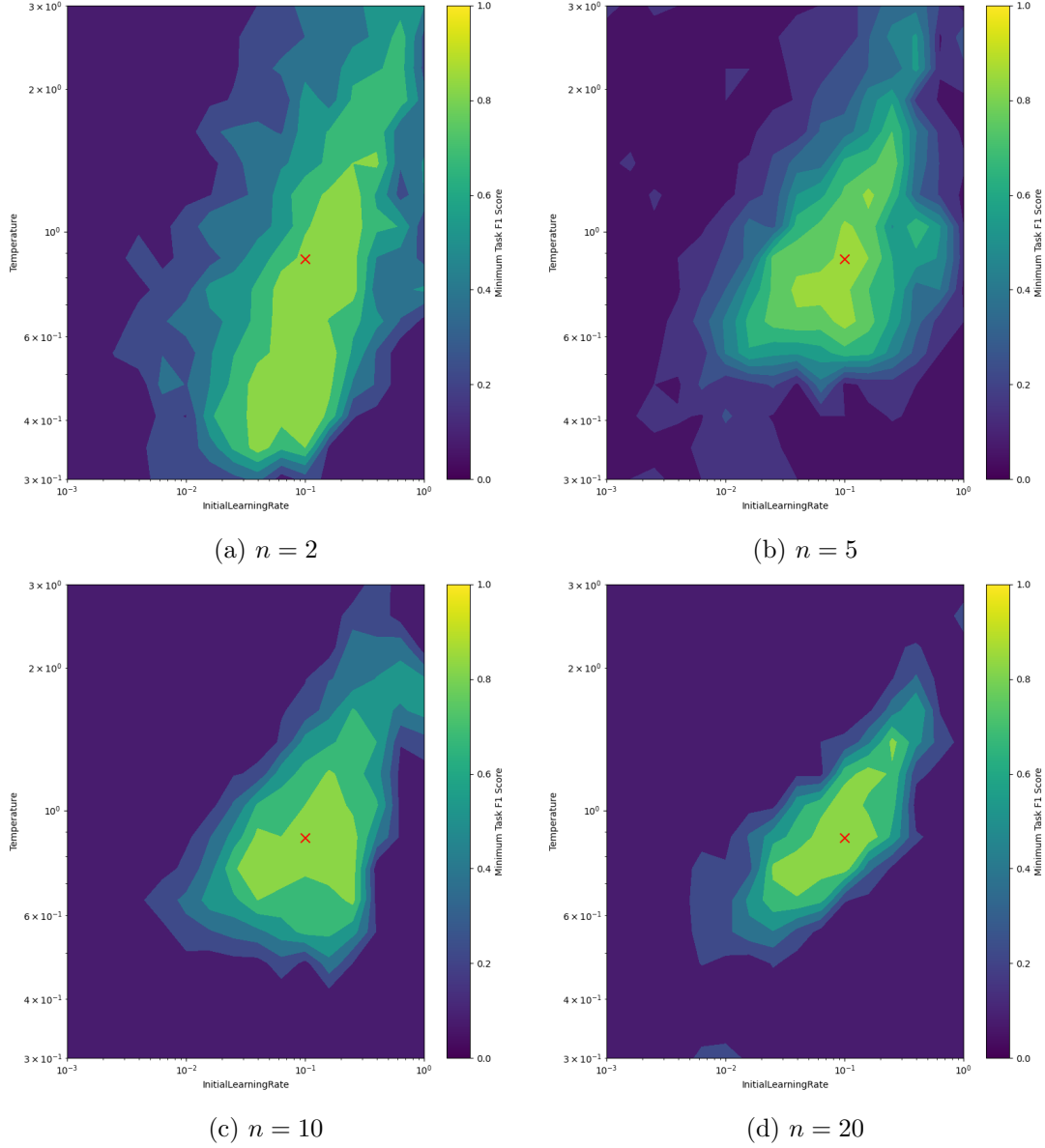


Figure 10: General network hyperparameter search on five Permuted MNIST tasks, measuring the minimum F1 score on the validation data. A larger minimum F1 score corresponds to a better performing network. The red cross indicates our choice of hyperparameters  $\text{lrInit} = 1 \times 10^{-1}$  and  $\frac{1}{\beta} = T_i = T_f = 0.875$ .

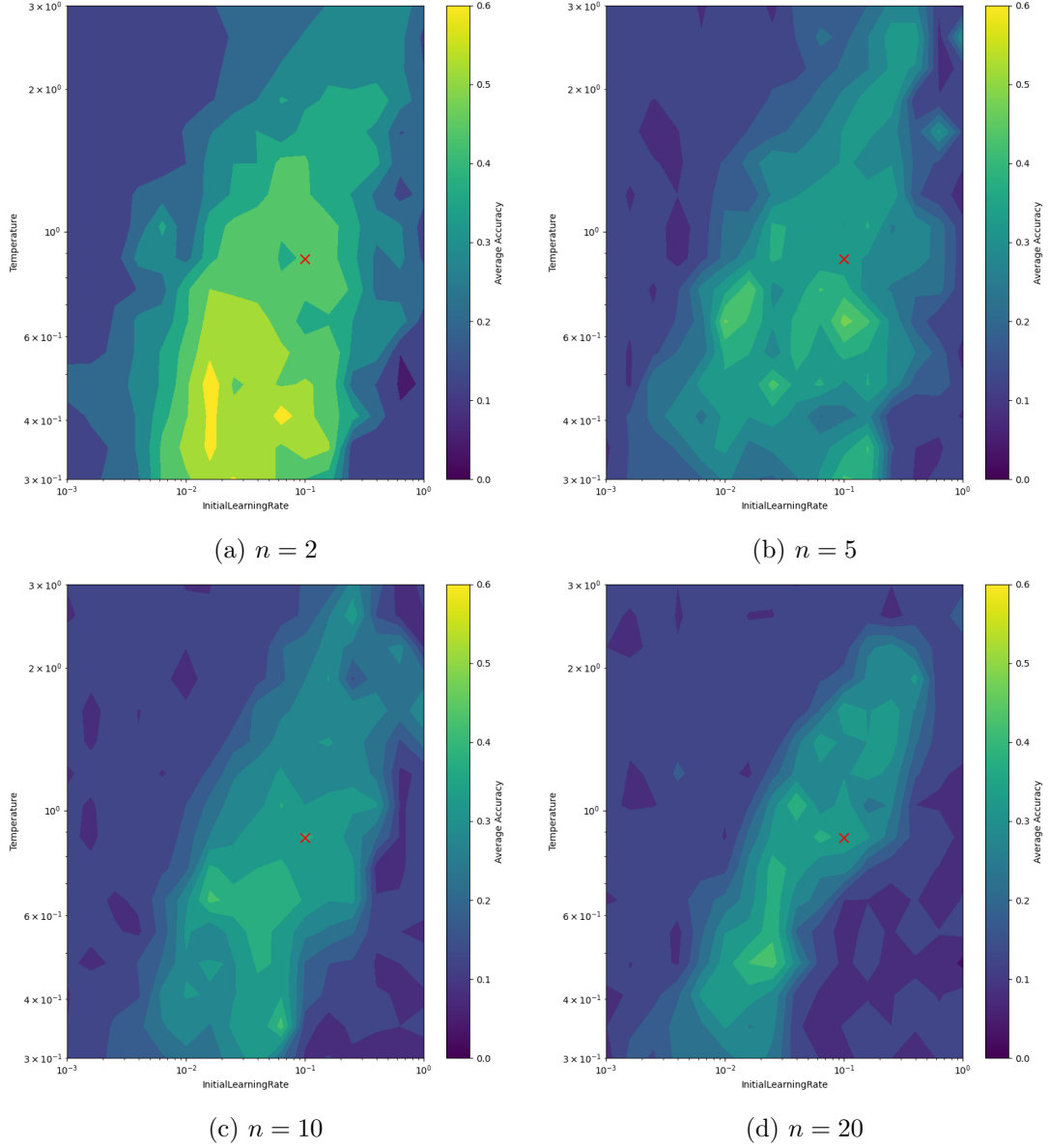


Figure 11: General network hyperparameter search on five Permuted MNIST tasks, measuring the average accuracy on the validation data. A larger average accuracy corresponds to a better performing network. The red cross indicates our choice of hyperparameters  $\text{lrInit} = 1 \times 10^{-1}$  and  $\frac{1}{\beta} = T_i = T_f = 0.875$ .